

Review

Experimental Challenges and Modelling Approaches of Floating Wind Turbines

Mohamad Hmedi ^{1,2}, Emre Uzunoglu ¹, Chen Zeng ¹, J. F. Gaspar ¹ and C. Guedes Soares ^{1,*}

¹ Centre for Marine Technology and Ocean Engineering (CENTEC), Instituto Superior Técnico, Universidade de Lisboa, 1049-001 Lisbon, Portugal;

mohamad.hmedi@ec-nantes.fr or mohamad.hmedi@centec.tecnico.ulisboa.pt (M.H.);

emre.uzunoglu@centec.tecnico.ulisboa.pt (E.U.); chen.zeng@centec.tecnico.ulisboa.pt (C.Z.);

jose.gaspar@centec.tecnico.ulisboa.pt (J.F.G.)

² Laboratoire de recherche en Hydrodynamique, Énergétique et Environnement Atmosphérique, CNRS UMR 6598, École Centrale Nantes, Nantes Université, 44321 Nantes, France

* Correspondence: c.guedes.soares@centec.tecnico.ulisboa.pt

Abstract: This paper reviews experimental methods for testing floating wind turbines. The techniques covered include early-stage and up-to-date approaches such as a porous disc method and hybrid model testing. First, the challenges induced by Froude and Reynolds similitudes and the importance of the various aerodynamic phenomena are discussed. The experimental methods are evaluated based on their cost, versatility, requirements, and limitations. The work primarily focuses on representing aerodynamic loads via hybrid and physical rotor testing, and a preliminary classification is proposed to facilitate the selection of the approaches. The work does not aim to identify an optimal method, but it provides insights into each method's distinctive features, serving as a roadmap for selecting the most appropriate methodology based on the specific testing goals and level of accuracy. Overall, this study offers a comprehensive resource for testing the coupled hydrodynamic and aerodynamic performance of floating wind turbines. The conclusions offer guidance for selecting an appropriate methodology based on the desired testing outcome.

Keywords: floating wind; wave tank testing; software in the loop; low Reynolds blades; drag disc; hybrid testing



Citation: Hmedi, M.; Uzunoglu, E.; Zeng, C.; Gaspar, J.F.; Guedes Soares, C. Experimental Challenges and Modelling Approaches of Floating Wind Turbines. *J. Mar. Sci. Eng.* **2023**, *11*, 2048. <https://doi.org/10.3390/jmse11112048>

Academic Editor: Constantine Michailides

Received: 25 June 2023

Revised: 15 October 2023

Accepted: 20 October 2023

Published: 25 October 2023



Copyright: © 2023 by the authors. Licensee MDPI, Basel, Switzerland. This article is an open access article distributed under the terms and conditions of the Creative Commons Attribution (CC BY) license (<https://creativecommons.org/licenses/by/4.0/>).

1. Introduction

Fossil fuel-based power plants are environmentally harmful and accentuate global warming. With the increase in energy demand and the intricate political status, the shift towards renewable resources becomes more crucial [1], which reflects the good economic prospects for the use of this type of energy [2]. To date, wind energy covers 35% of renewables in Europe, with the majority of wind turbines (WTs) situated on land [3]. While the conventional deployment mode is onshore, implementing WTs in offshore locations is more efficient. The move to offshore utilization is driven by favourable wind regimes at these locations, specifically higher wind speeds and reduced turbulence. In addition, the visual, environmental, and auditory impact of offshore WTs is lower compared to onshore installations, making them a reasonable choice for larger turbine deployment. Overall, the benefits of offshore WTs deployment make it a viable option for renewable energy generation [4].

Recent years have witnessed a marked trend towards the utilization of offshore locations for the deployment of WTs [1]. When water depth exceeds 50 m, floating structures are deemed the most appropriate option. Recent analyses have shown that bottom-fixed offshore wind turbines are financially infeasible above 50 m depth due to the high expenses incurred for installation [5,6]. By contrast, floating wind turbines (FWTs) have demonstrated better economic viability in deeper waters [7,8]. In this context, several designs have

been developed, including tension leg platforms (TLPs), semi-submersibles, and spar-type structures [9]. These designs are inspired by the oil and gas industry and intend to support WTs under a coupled wind and wave excitation.

Given the complexity of the environment, the investigation of conceptual design dynamics is necessary to guarantee their operational capabilities. Various initiatives, both industrial and academic, have been undertaken to progress the state of the art in floating wind technology. Notable examples of implemented prototypes include Blue H TLP in Italy [10], Statoil's Hywind Spar in Norway [11], WindFloat semi-submersible in Portugal [12], and FLOATGEN barge in France [13]. These designs were mostly developed through a collaborative effort between industry and academia. LIFES50+ [14,15], INNWIND.EU [16], and ARCWIND [17] exemplify the interdisciplinary cooperative research between academia and industry in advancing floating wind technologies.

The collaborative work for floating wind projects follows a series of stages guided by the Technology Readiness Levels (TRLs) [18,19]. The first stages (i.e., TRLs 1–6) integrate both numerical simulations and experimental testing to validate the concept. Numerical tools involve mathematical models and computer algorithms to estimate the physical properties and foresee the behaviour of the floating turbine. Design tools (e.g., ParMod [20,21]) and simulation software (e.g., OpenFast [22], Qblade [23]) offer the advantage of exploring a wide range of parameters and testing various wind and wave scenarios. Meanwhile, experimental testing provides a higher degree of accuracy and reliability based on direct measurements of the system. Additionally, experiments can reveal unexpected phenomena or behaviours that may have been ignored by simulations, such as neglecting viscous effects in potential flow calculations [24] and the coupling between aerodynamics and hydrodynamics. Therefore, complementing the numerical simulations with experimental testing validates the mathematical predictions and provides a more comprehensive understanding of the system.

To validate the theoretical predictions and the design dynamics, experimental testing is necessary, particularly in areas where the theory falls short. Building scaled models for hydrodynamic testing in a wave tank requires satisfying Froude (Fr) similitude conditions [25–27]. Nevertheless, the Reynolds number (Re) is decreased, and thereby the aerodynamic performance of the turbine is altered [28]. Accurately modelling mass (gravity and inertia) and mooring loads introduce further challenges to the testing environment. Furthermore, given the interplay between the turbine's aerodynamics and the blade pitch controller [29], incorporating the controller is generally not overlooked. Blade pitch control strategies for onshore turbines induce negative aerodynamic damping effects when used for floating wind systems (i.e., the motion is amplified rather than dissipated) [30–34]. A noticeable effort is visible in testing and validating new control strategies for FWTs [35–37]. Therefore, testing the concept considering the coupling between all components is needed, where both Fr and Re quantities are conserved.

The need for a testing environment that respects both Fr and Re poses a challenge for FWT experimental campaigns. To overcome the Fr – Re scaling conflict, different methodologies have been adopted to represent the aerodynamics of the turbine. The earliest techniques involved static cables that represent steady wind loads [38] or a drag disc to replicate the rotor thrust [39–41]. Froude-scaled rotors (FSRs) were used with high wind speeds to match the turbine's thrust in the below-rated speed zone [42–44]. Given the necessity for higher wind speed, performance-scaled rotors (PSRs) (i.e., a redesigned rotor with an identical aerodynamic performance of the turbine at a lower Re number) were then utilized [45–52]. The requirement of a wind generating system above the wave tank, which is uncommon, paved the way to develop hybrid-testing approaches. The hybrid methodology combines physical testing and numerical simulation in real-time. An actuation system provides the coupling between the simulated WT and the physical floater in the wave basin [53–62] or inversely in the wind tunnel [63–65].

Considering the variety of approaches to replicate the turbine's aerodynamics, each has its advantages and limitations, with some being more adequate than others in some

cases. This paper provides an overview of these methods, their strengths, and weaknesses. First, Froude and Reynolds scaling are reviewed, followed by the test’s sensitivity to various aerodynamic phenomena. The experimental techniques are then detailed and evaluated based on their cost, versatility, requirements, and limitations. The comparison between the different methods mainly focuses on hybrid and physical rotor testing. The various methods are organized to achieve that goal, and a preliminary classification is proposed. The primary objective is to present an overview that compares the existing methods while providing insightful observations on their distinctive features. It should be noted that the ultimate aim is not to determine the “best” technique but rather to furnish a means of comparing the different methods. The conclusion provides a roadmap for selecting the suitable methodology based on the experiment’s goal.

2. Froude and Reynolds Similitude

The Froude number is a dimensionless quantity used to indicate the influence of gravity on a fluid’s motion:

$$Fr = \frac{U}{\sqrt{gL}} \tag{1}$$

while the *Re* number is the ratio of inertial forces to viscous forces:

$$Re = \frac{\rho UL}{\mu} = \frac{UL}{\nu} \tag{2}$$

where *U* is the wave (fluid) celerity, *L* is the characteristic length, *g* is the gravity acceleration, ρ is the fluid density, and μ and ν are the dynamic and kinematic viscosity, respectively.

The geometric scaling between the full (*f*) and model (*m*) scale environments is as follows:

$$L_f = \lambda L_m \tag{3}$$

where λ represents the scaling factor.

To ensure the hydrodynamic similitude (i.e., conserving the gravitational loads), the *Fr* number is kept constant between both scale environments:

$$Fr_f = Fr_m \tag{4}$$

Table 1 presents the Froude-scaling factors for some parameters for a constant fluid density. For a detailed understanding of the scaling methodology see [66].

Table 1. Scaling factors for some parameters using Fr similitude.

Parameter	Units	Factor
Length	m	λ
Time	s	$\sqrt{\lambda}$
Volume	m ³	λ^3
Force	N	λ^3
Moment	N·m	λ^4
Power	W	$\lambda^{7/2}$
Inertia	kg·m ²	λ^5
Angle	Rad	1

The velocity and time relationships according to Fr scaling are as follows:

$$U_f = \sqrt{\lambda} U_m \rightarrow t_f = \sqrt{\lambda} t_m \tag{5}$$

while for *Re* scaling, they are related as follows:

$$U_f = \frac{U_m}{\lambda} \rightarrow t_f = \lambda^2 t_m \tag{6}$$

From Equation (5), if *Fr* similitude is applied, the relation between the full and model scale *Re* numbers is as follows:

$$Re_f = \lambda^{3/2} Re_m \tag{7}$$

Equation (7) demonstrates a lower *Re* number at the model scale where *Fr* similitude is applied. For instance, the *Re* number is reduced by a factor of 350, nearly three orders of magnitude, for a 1/50 *Fr* scaled model, as seen for the DeepCwind semi-submersible testing [67,68]. Applying *Fr* scaling to the floater and *Re* scaling to the rotor is limited, with the need for ferocious wind speeds at the model scale and difficulties with scaling down time. For instance, if the geometric scaling factor (λ) is 30, a wind speed of 300 m/s is required over the basin to represent a 10 m/s Re-scaled wind, and one second Re-scaled period represents 900 s at full scale (Equation (6)).

3. Significance of Aerodynamic Phenomena

FWTs experience environmental loads throughout their lifetime, classified into hydrodynamic, aerodynamic, and inertial loads (Figure 1). The equation of motion that governs the behaviour of an operational FWT, following Newton’s second law, can be expressed as follows [69]:

$$[M + A]\ddot{\vec{x}} + B\dot{\vec{x}} + [C_h + C_m]\vec{x} = \vec{F}_{ex} + \vec{F}_{aer} + \vec{M}_{gyr} \tag{8}$$

where \vec{x} , $\dot{\vec{x}}$, and $\ddot{\vec{x}}$ are the system’s motion, velocity, and acceleration tensors. *M* represents the mass and inertia matrix, *A* is the added mass matrix, *B* is the damping matrix, *C_h* is the hydrostatic stiffness matrix, *C_m* is the mooring stiffness. \vec{F}_{ex} the incident wave excitation force, \vec{F}_{aer} is the total aerodynamic tensor, and \vec{M}_{gyr} are the gyroscopic moments. As the methods discussed in the paper focus on replicating the turbine’s aerodynamics, the following presents the importance of different aerodynamic phenomena on the responses of an FWT.

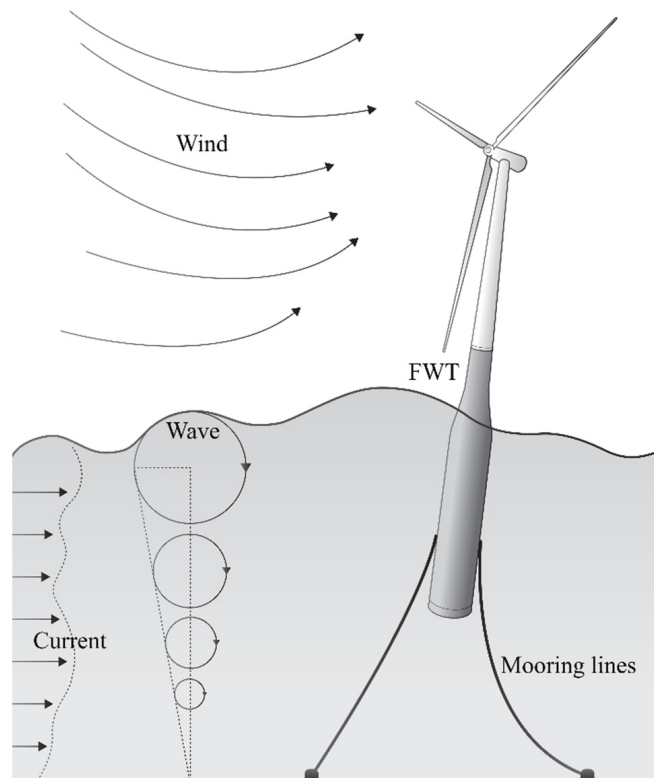


Figure 1. Floating wind turbine subjected to various loads.

3.1. Aerodynamic Loads

The aerodynamic conversion process at the rotor creates in the hub frame an aerodynamic tensor of six components [70]:

$$\vec{F}_{aer} = [F_x; F_y; F_z; M_x; M_y; M_z] \tag{9}$$

The thrust force F_x dominates the two force components F_y and F_z . The generator torque M_x also dominates the local aerodynamic pitch and yaw moments (i.e., M_y and M_z). A load sensitivity analysis is made by eliminating the non-dominating aerodynamic forces and moments when simulating a semi-submersible FWT [70]. It is concluded that M_y affects the platform pitch motions and mooring line tension with 10–15% changes in the standard deviation are seen. M_z has significant effects on the yaw response (i.e., 2–10% in the parked case), and is usually small and excited at low frequency. If torsional responses is not aimed, M_z can be neglected for operational scenarios [70]. F_y influences the sway motion, roll motion, and tower side–side bending moment, which are typically smaller than the corresponding surge, pitch, or fore–aft bending moment. F_z has a negligible effect on the platform motions in operational conditions. However, F_z affects by up to 15% the surge, pitch, and yaw motions for parked conditions and misaligned wind–wave conditions.

In addition, wind turbine controller settings modify the platform’s dynamics. The controller adjusts the blade’s pitch angle and the generator torque, which alters the aerodynamic loads [29]. Platform pitch instabilities may be induced if a land-based controller is used for FWT [30]. To prevent instabilities, FWT-specific control strategies are developed [32,71,72]. Thus, emulating the controller during the tests allows the replication of the coupling effect between the controller, aerodynamics, and the system dynamics.

3.2. Inertial Loads

In addition to the aerodynamic loads, inertial loads are produced due to the rotation of the blades. The centripetal acceleration of the rotor results in an inertial centrifugal force. Each blade element with a mass dm and flapping angle β , located at a distance r from the blade’s root-end, is subjected to a centrifugal force dF_c along the chord direction [73]:

$$dF_c = r \omega_r^2 dm \cos \beta \tag{10}$$

For perfectly symmetric blades, the total centrifugal force would be zero. However, as the blades are unbalanced, a small resultant force will be generated periodically at the rotor speed (i.e., 1P frequency).

Moreover, any rotational motion of the platform will produce a gyroscopic moment due to the rotor’s rotation. For instance, a platform pitch motion induces a yaw moment for a horizontal axis WT. The gyroscopic moment is defined as follows [74]:

$$\vec{M}_g = J_r \vec{\omega}_r \wedge \vec{R}_p \tag{11}$$

with J_r is the rotor inertia, $\vec{\omega}_r$ is the rotor’s rotational speed, and \vec{R}_p corresponds to the platform rotational speed vector.

The sensitivity analysis conducted on a semi-submersible demonstrates that the gyroscopic moments and centrifugal forces primarily affect the sway, roll, and yaw motions up to 5% in operational conditions [70]. Disregarding the gyroscopic effects for a spar FWT overestimates the tower torsion up to 17% [75].

3.3. Loads Frequency Bandwidth

The excitation loads are distributed along a frequency bandwidth [40,53,76]. In experimental testing, the loads should be emulated with the correct amplitude and frequency content. Table 2 exemplifies the bandwidth for the OC3, OC4, and the triple spar models [53], explained as follows:

- The low frequency (LF) range may coincide with the natural frequencies of the FWT along the 6 degrees of freedom (DoF). It should be noted that TLPs have high natural frequencies in heave, roll and pitch as the moorings increase the system stiffness [5,21].
- The wave frequency (WF) range exciting the platform motions.
- The 1P and NP rotor frequencies range corresponding to the frequency of one full rotation of the rotor and the frequency at which one blade among N blades passes in front of the tower. NP would be referred to as the 3P frequency for a three-blade WT.
- The first fore–aft and side–side tower bending mode (Twr 1st).
- The high frequency (HF) range, including the blade modes (flapwise and edgewise).

Table 2. Limits of the frequency bandwidths at full scale.

	LF	WF	1P	3P and Twr 1st	HF
Low limit (Hz)	0.005	0.04	0.12	0.4	0.8
High limit (Hz)	0.05	0.25	0.2	0.8	2

4. Early-Stage Methods

Wave tank experiments were first performed to gauge the performance of FWTs. This section summarises the earliest testing campaigns, including the methodologies (i.e., the drag disc and static cables), strengths and weaknesses of each approach, and suggestions for improving their effectiveness.

4.1. Static Cables

The static cable approach was initially employed by Utsonomiya et al. [38] to evaluate the performance of a spar design. The main goal was to replicate the static tilt of the platform correctly under wind loads coupled with hydrodynamic loads from waves. The method involves using a cable (Figure 2) to imitate a static thrust obtained from the thrust curve of a given turbine. During Utsonomiya’s campaign, decay, regular and irregular wave tests, and regular wave tests with a steady rotor thrust applied at the tower’s top via the cable were conducted. However, only a steady thrust force was considered, neglecting other aerodynamic loads and interactions such as wind turbulence, aerodynamic damping, controller effects, and gyroscopic moments.

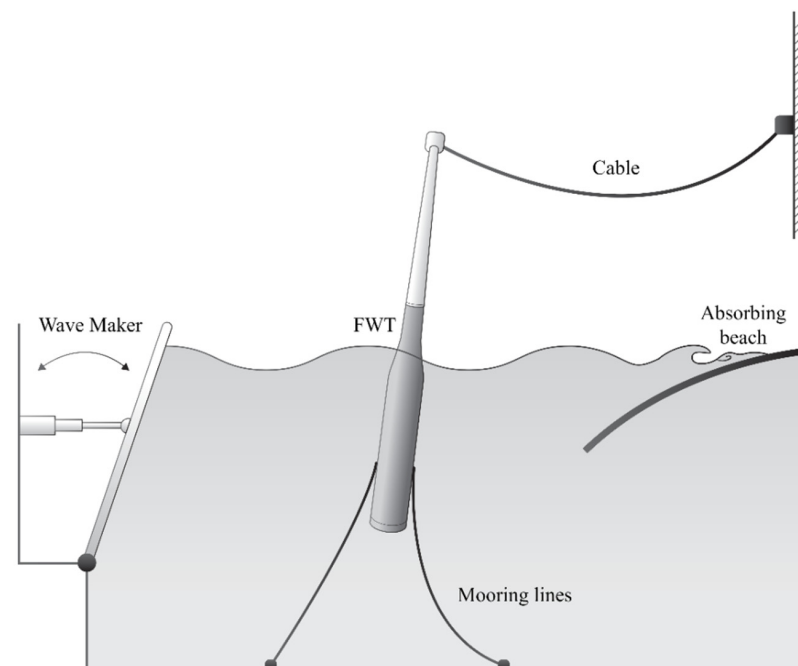


Figure 2. Static cable approach.

Although this approach is simple and quick, it lacks variability as it reproduces only a steady thrust force without considering the wind turbulence and the controller effects. Additionally, using the thrust curve of the WT does not account for the platform response in the calculation of the aerodynamic load, and the gyroscopic effects are not considered. Furthermore, this technique ignores other aerodynamic load components, such as aerodynamic moments and the coupling with the blade pitch controller. In other words, testing with a static cable is limited to steady wind cases where the rotor thrust is relatively constant.

One possible improvement to this method is to connect the cable to a dynamic winch that can vary the tension instantaneously to match the thrust force obtained in a real-time simulation of the turbine. This adaptation would convert the approach into a “Software in the Loop” (SIL) system described in Section 5. Another enhancement is using a rotating disc to reproduce gyroscopic moments [12]. Despite its limitations, this method remains a valuable and straightforward approach for investigating the hydrodynamic response of FWTs under steady wind loads [77].

4.2. Porous Disc

One possible method for reproducing the turbine thrust involves replacing the rotor with a drag/porous disc exposed to an airflow (Figure 3). For FWTs, the use of this technique has been documented in several research papers, including the 1:105 [12,39] and 1:67 [40] scale WindFloat semisubmersible, as well as combined FWT-wave energy converter (WEC) systems [41,78,79].

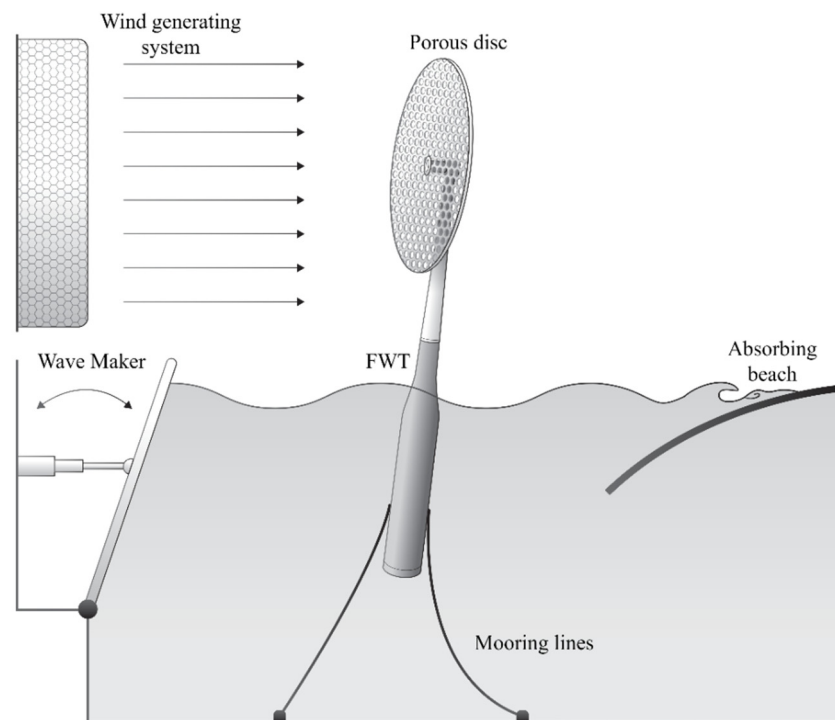


Figure 3. Porous disc approach.

The drag disc method boasts a high degree of versatility and ease of implementation for various turbines. The construction and calibration processes are relatively straightforward, highlighting the method’s practicality. Additionally, the method yields a consistent thrust force compared to the thrust curve in the below-rated zone, which is beneficial when testing wind turbines in wave tanks. The ability to generate wind loads below the rated wind speed is particularly noteworthy, as it allows for comprehensive testing under controlled conditions. In general, the drag disc method offers a compelling option for FWT testing when a wind-generating system is available.

Despite its use for FWT testing, the porous disc approach has considerable drawbacks. One notable issue is the method's failure to account for the gyroscopic moments, the aerodynamic yaw and pitch forces and moments and the generator torque [41]. In addition, the vortex shedding generated by the disc can cause vibrations that add more uncertainty to the measurements. Furthermore, this technique is limited in applicability since it cannot accurately simulate wind loads in the above-rated wind speed zone. Once the wind speed exceeds the rated level, the generated thrust force will surpass the expected value from the thrust curve, resulting in an incorrect emulated thrust. Attempting to simulate a control system using the drag disc method is not feasible, so it fails to account for the coupling between aerodynamics and the controller.

Consequently, it is unsuitable for testing control strategies and prevents varying the thrust coefficient, leading to incorrect aerodynamic damping. The need for a wind generating system increases the test operating costs as such wind blowers are both expensive to operate and not commonly available over the basin, which creates a barrier to the widespread adoption of this method. Finally, a light disc is advisable to maintain a margin for calibrating the system's mass properties. While the WindFloat campaign has attempted to address some limitations (i.e., using a spinning disc to replicate gyroscopic effects [12,39]), the drag disc approach is still partially bounded, with several notable deficiencies.

5. Physical Rotor

5.1. Froude-Scaled Rotors

An obvious option for replicating the aerodynamics of FWTs is to use a Froude-scaled rotor (FSR) in the experiment (Figure 4). In 2007, Marintek ocean basin laboratory (currently SINTEF) evaluated a 1:67 scaled model of the Hywind Spar with an FSR. In their campaign, two DC motors served to set a constant blade pitch angle and the rotor's rotational speed [31,33]. Likewise, the AAUE-TLP fitted with an FSR of the NREL 5 MW WT and underwent testing at Aalborg University, where the generated wind speed was amplified to reproduce the thrust force correctly [80]. A similar approach was adopted by Ahn and Shin [81] to examine the dynamics of the Hywind Spar. In a study by Bahramiasl et al. [74], in which the wind speed was also increased, a 1:100 Sea-Star TLP model was examined to investigate the gyroscopic effects at different wind headings. In the same campaign, a motor initiated the rotor's rotation due to mechanical friction blocking the rotation from the blowing wind. In another investigation by Wen et al. [82], an FSR was utilized to evaluate the aerodynamic loading effects on the JTU-S4 spar model. Michailides et al. [43] investigated the performance of a combined wind-wave energy concept (SFC) in extreme conditions. They used an FSR calibrated in a wind tunnel to obtain the expected thrust for varying wind speeds and blade pitch angles.

A notable campaign is the DeepCwind in 2013 [42,44,83] at MARIN, where three FWT systems (Sea-Star type TLP [84], Hywind spar [85], DeepCwind semi-submersible [86]) were scrutinized. It brought the first floating offshore wind data available to the public and allowed others to learn from the issues that arose during their tests. The data collected from this campaign validated the numerical model of the three designs [68,87,88]. In DeepCwind tests, an FSR was used, and the wind speed was amplified to reproduce the rotor's thrust force accurately. For instance, a 21.8 m/s blowing wind was utilized to replicate the rated wind speed scenario of 11.4 m/s.

A significant shortcoming of increasing the wind speed is the generation of unwanted loads on the tower and the platform. Moreover, to prevent interaction with the waves, the fans were placed high enough with the nozzle tilted 2.16 degrees downward. The inclination of the nozzle introduced a vertical component of the wind velocity, resulting in a 20% reduction in the wind speed at the lower ends of the rotor. Furthermore, the generator torque was not accurately replicated, and the motors induced the blades' rotation. The blade pitch angle remained constant throughout all the tests as no control system was used. The lack of a controller and the need for higher wind speed made above-rated wind conditions infeasible for testing.

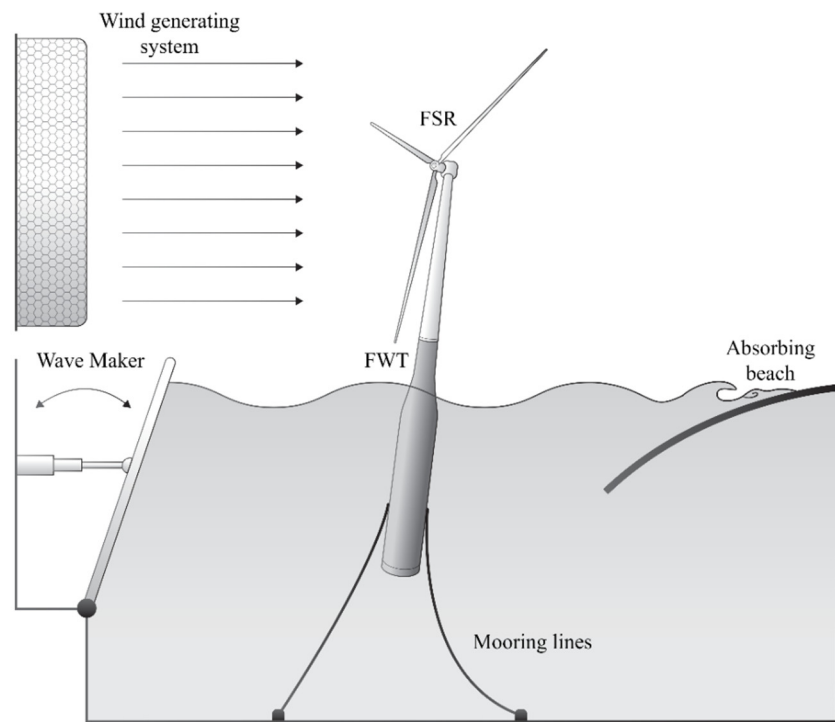


Figure 4. Froude-scaled rotor approach.

The results from these campaigns conclude the need for adjustments and modifications in future studies to replicate the aerodynamic loads accurately. It was suggested to use a performance-scaled rotor (PSR), where the blades are redesigned for a similar performance at low Re [42]. In addition to PSRs, attempts were made to tackle the limitations of this approach. In studies by Li et al. [89] and Duan et al. [47], a modified version of FSR was employed. The DeepCwind semi-submersible [88] and the Hywind spar [47] were the tested platforms, and the adjustment made was to let the rotor freely spin instead of using a motor to initiate the rotation. The motor was devoted as a generator to decelerate the rotor speed, and the tip speed ratio (TSR) was correctly kept to some extent. The improvement resulted a marginally increased wind speed compared to the initial version, such as using 12.8 m/s wind speed instead of 21.8 m/s for the rated scenario (i.e., 11.4 m/s).

5.2. Performance-Scaled Rotor

Following the conclusions of the DeepCwind campaign in 2013 [42], efforts were made to construct performance-scaled rotors (PSRs) [50,83], where the blades are redesigned for a low Re environment (Figure 5). Accordingly, the DeepCwind semi-submersible was retested with a PSR at MARIN [90,91]. The new testing campaign validated the results obtained in the first campaign, where the global performance was roughly identical. On the other hand, the new concept allowed the performance of new tests that were not feasible by the FSR. For instance, the above-rated wind speed tests were made, and the potential implementation of an active blade pitch controller was considered to investigate the controller's impact on the global performance of the floating turbine.

A MARIN PSR was used again to test the GustoMSC Tri-Floater, and the measured thrust matched the full-scale turbine predictions. The Windstar TLP [92] mounting the NREL 5 MW was tested using a PSR at the SKLOE laboratory (i.e., Shanghai Jiao Tong University) and demonstrated the effectiveness of this approach in resolving the scaling problem. PSR is utilized to test larger turbines such as the DTU 10 MW WT [93]. Among the tests found in the literature are the triple Spar model [94] and the sea-star TLP [95] at DHI Denmark. Using a PSR, an upscale of the DeepCwind semi-submersible with the DTU 10 MW underwent testing in the INNWIND.EU project at LHEEA—Ecole Centrale de Nantes (ECN) [16,96]. The University of Ulsan (UOU) 10 MW design [97], the KIER

TLP [98], and the EOLINK TLP [99] exemplify the wide use of the PSR method. Technical details and information on how the blades are designed and fabricated are out of the scope of this paper and can be found in references [28,51,100].

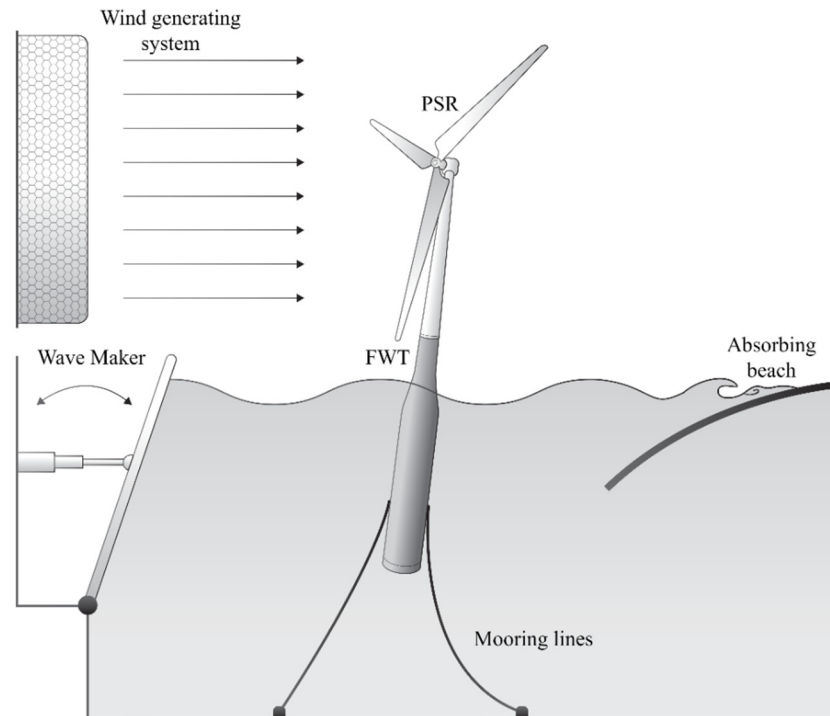


Figure 5. Performance-scaled rotor method.

The PSR approach brought several advantages, improving the fidelity of the experiments. A correct thrust force coefficient in a Froude-scaled environment could be maintained, as well as the TSR. In addition, the ability to implement and test wind turbine controllers is possible. The rotor torque, the aerodynamic damping, and gyroscopic moments can be replicated, along with other unexpected aerodynamic and hydrodynamic phenomena uncaptured by some numerical tools.

However, emulating physical wind over a wave tank requires a wind generation system, making PSR costly to adopt and operate [101]. Calibration of the wind speeds, wind gradient and turbulence increase the complexity of the experimental setup. The accuracy of the wind generation systems over the basin is much less than in wind tunnels. For instance, in most campaigns (e.g., [42,96]), multiple fans pumping the air through ducts and honeycomb mesh were used. The difficulty of controlling the boundaries of airflow after exiting the nozzles was noticed in most campaigns [46,98]. Thus, the ability to replicate the same test decreases, adding more uncertainty to the measurements. Moreover, the low Reynolds number at the model scale leads to inaccurate modelling of the WT's power and torque coefficients. The methodology has shown a good representation of the real scheme of a wind turbine. However, less versatility is present as each turbine has a specific blade geometry, and a redesigned blade for each turbine design and scaling factor is needed.

6. Hybrid Testing

Hybrid testing emerges as a sophisticated technique that synergistically combines physical testing and numerical simulation, fostering a holistic approach to experimentation. The inception of this approach originates back to the 1970 s in the field of earthquake engineering [102]. In that context, the technique was pioneered to investigate the dynamic response of structures subjected to earthquake conditions. The procedure involved compu-

tationally determining the structure's displacements and subsequently applying them in real-time to the physical model using multiple actuators.

FWTs tests borrowed the approach, drawing inspiration from the aforementioned concept. Similarly, the system's motions can be reproduced using a robot in a physical wind environment [64], or the aerodynamic loads can be emulated under physical wave conditions using actuators such as cables, propellers, or ducted fans [62,103]. The simplest version involves emulating a pre-recorded time series of motions or aerodynamic loads through the actuation system. However, synchronising the wave elevation with the emulated aerodynamic loads (or the blowing wind with the robot motions) poses a challenge. Furthermore, the real-time replication of blade pitch controller effects remains elusive. Additionally, the fidelity of these tests is constrained as the simulation fails to account for the platform's actual (i.e., the measured) motion in the underlying calculations.

A higher fidelity hybrid technique with increased complexity is developed to address these limitations. This approach entails the real-time integration of physical testing and numerical simulation. In the cases where an actuator replaces the rotor, the platform's motions are tracked and subsequently fed into a numerical tool. The simulation provides the aerodynamic loads considering the platform motions at each corresponding time step, which are then appropriately scaled and replicated by the actuator [54].

In a study conducted by Stewart and Muskulus [104], a comparison is made between utilizing pre-calculated time series of aerodynamic loads and real-time testing. The findings indicate that employing predefined loads results in significantly larger discrepancies in both loads and motions when comparing the simulation to the experimental data. This discrepancy arises from the absence of a feedback loop between the system's motions and the predefined aerodynamic loads. However, implementing real-time testing introduces challenges associated with compensating for delays [103].

This methodology is referred to by various names, such as "Software in the Loop" (SIL), "Hardware in the Loop" (HIL), and "Real-Time Hybrid Model" (ReaTHM) testing. All of these terms encompass tests that combine physical testing and numerical simulation. In general, this integration offers substantial benefits for testing complex structures like FWT. However, it necessitates meticulous compensation for delays to enable swift actuator execution within small time steps. Note that a similar approach is adopted in ocean engineering to test mooring line dynamics. The motions of a floating platform under wave excitation are measured experimentally and used in numerical simulations of the full-scale mooring lines [105–109]. The following section provides a comprehensive overview of the hybrid testing campaigns conducted on FWT and highlights the distinct advantages offered by each actuation system employed in these tests.

6.1. Propeller Actuators

When considering the selection of actuators for hybrid testing, researchers have utilized various options such as propellers, ducted fans, and cables. Among these choices, propellers and ducted fans have emerged as more commonly employed. Azcona et al. [54] utilized a ducted fan positioned at the hub height to replicate the rotor's thrust (Figure 6). The thrust force was calculated in real-time by the numerical tool FAST [110], which received the platform motions obtained from the basin measurement. The strategy was applied to test a 1:40 scale model of the OO-Star semi-submersible [15] equipped with a 6 MW wind turbine at the ECN wave basin. The successful implementation of this campaign demonstrates the SIL's capability to incorporate aerodynamic damping. The same principle was applied at the ECN basin to test the DeepCwind semi-submersible with the NREL 5 MW WT [61,111] and the DTU 10 MW WT [96]. Notably, an improvement was made by incorporating second-order hydrodynamics into the numerical model, enhancing the fidelity of the simulated load and the tests.

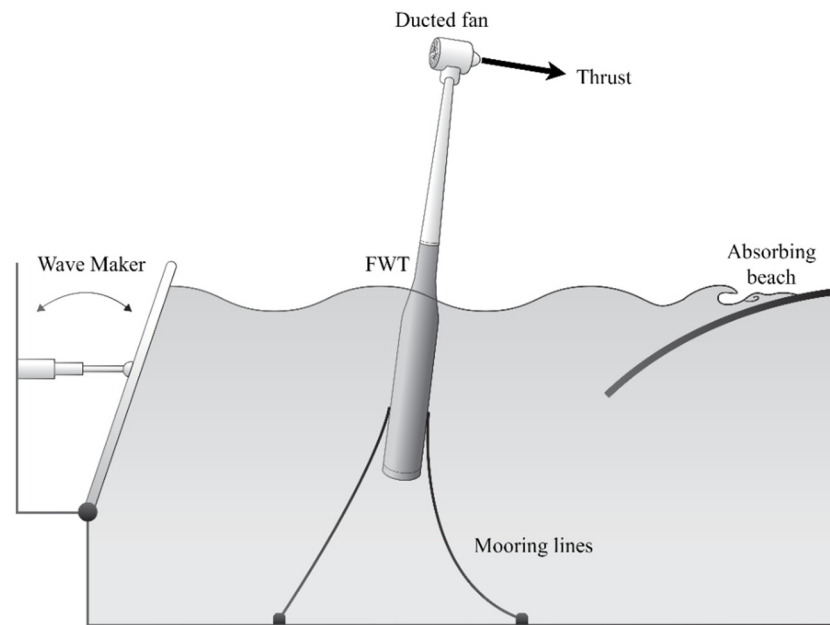


Figure 6. Hybrid testing using a ducted fan.

In addition to these SIL systems, numerous researchers have widely adopted the hybrid approach using ducted fans or propellers. Desmond et al. [112] employed a simplified version of the hybrid technique to evaluate the SCDnezy2 semi-submersible, which supports two 7.5 MW WT. In that campaign, two ducted fans substituted the two rotors and generated steady wind loads of up to 10 N thrust on each tower. Similarly, Wright et al. [113] utilized a single ducted fan generating steady thrust to test a hexagonal TLP design in two scales. Andersen [114] employed a ducted fan to emulate a recorded time series of thrust to test a three-column semi-submersible.

However, emulating recorded loads is low fidelity compared to SIL since they do not replicate the blade pitch controller effects in real-time, and the instantaneous motions are not considered in the simulation of aerodynamic loads. A comparison between hybrid testing with and without SIL (i.e., real-time exchange between the simulation and the physical testing) was conducted by Matoug et al. [115]. The NAUTILUS semi-submersible [14] with the DTU 10 MW [93] and the WindQuest 10 MW [116] were tested, revealing a 14% improvement in cross-correlation between numerical simulation and experimental testing when SIL is employed.

Building upon these findings, implementing single propeller actuators with SIL has been extensively utilized in various campaigns. For instance, the Iberdrola TLP [117] was tested at the Kelvin Hydrodynamics Laboratory (KHL) at the University of Strathclyde [118] using a single ducted fan and following the same SIL concept described by Azcona et al. [54]. The approach was also applied to test the SOFTWIND Spar [53,76,119] at ECN. However, it should be noted that the single fan actuator aims to reproduce the thrust force exclusively, and the other aerodynamic loads and gyroscopic moments are not emulated with a single actuator. Therefore, efforts have been made to develop multi-actuator systems capable of reproducing the full aerodynamic tensor.

As the first version only emulated the thrust force, Azcona et al. developed a new multi-propeller system capable of reproducing the rotor moments [120]. This concept improves the SIL system by incorporating the moments generated by the aerodynamic and gyroscopic effects. Within the ARCWIND project, the multi-propellers system is utilized to test the CENTEC-TLP [5,17,62,121] and the SATH10 semi-submersible [122]. At the Instituto Hidraulica Cantabria (IHC), an actuator consisting of six drone propellers is developed by Urbán and Guanche [60] and utilized to test the TELWIND FWT [123]. The propellers are calibrated and tuned to account for the aerodynamic influence resulting from their proximity. The results demonstrate small deviations compared to the theoretical values of

the loads. Another six-propeller actuator was developed by Otter et al. [59,124] at MaREI, Ireland, and exhibited good performance in emulating both thrust and torque. Additionally, a multi-propeller system was employed by Kanner et al. [125] to test a vertical-axis WT, expanding the application beyond horizontal-axis WTs.

6.2. Cable Winch Actuators

In addition to propellers and ducted fans, cable winches have been explored as actuators in hybrid testing. Early testing campaigns employed cables to replicate static thrust based on the turbine-specific thrust curves [38] (Section 4.1). However, to overcome the limitations of the static cable approach, researchers sought to improve the method by applying tensions instantaneously to the model based on real-time simulations. The underlying concept of using cable winches as actuators in hybrid testing is similar to the SIL system with propeller actuators.

One of the pioneering systems employing cable winches as actuators is developed at SINTEF in Norway. Their technique, known as ReaTHM testing, utilized six cables attached to a square frame at the hub height (Figure 7). Researchers at SINTEF employed this system to conduct experiments on the NOWITECH model, which featured the NREL 5 MW turbine [55–57]. To optimize the cable-based method, a sensitivity analysis was performed by Bachynski et al. [70], resulting in the emulation of a reduced number of aerodynamic loads based on the analysis outcomes. Further enhancements were introduced by Thys et al. [126] to encompass wind direction variability and tower loads, extending the frequency bandwidth to include the 3P frequency and the first tower bending frequency. The updated system was employed to test the NAUTILUS semi-submersible with the DTU 10 MW WT, with a comparative analysis against the previous system presented by Chabaud et al. [58]. The results indicate that the new system provides greater flexibility in replicating loads despite requiring higher cable tensions.

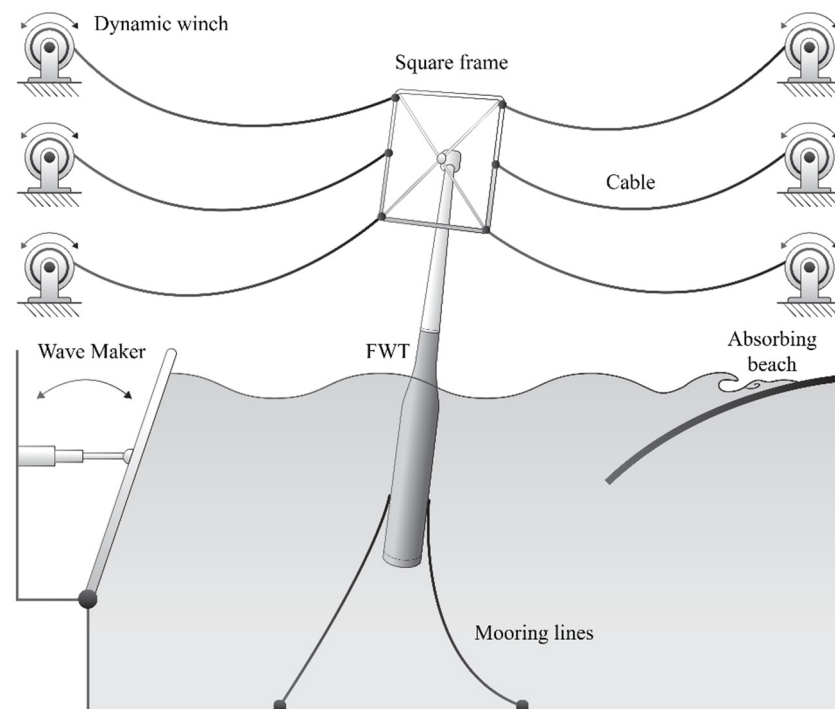


Figure 7. Hybrid testing using dynamic winches.

Another study by Antonutti et al. [127] utilized a similar hybrid system with cables to test a semi-submersible mounting of the Haliade 6 MW WT. Their system consists of five cables enabling actuation of the surge, pitch, and yaw degrees of freedom. The results demonstrate good agreement between the experimental and numerical models. Moreover,

a hybrid system employing cable actuators was used by Hall et al. at the University of Maine, USA, to test a 1:50 scale model of the DeepCwind semi-submersible [67,128]. Unlike other cable-based systems, their approach replicates only the thrust force. Two opposing cables attached to the turbine at the hub height are used as the actuator. The results obtained from this hybrid testing are compared to those of complete physical testing with a PSR [50] and reveal a satisfactory agreement, particularly regarding motions and mooring tensions. It also demonstrates the capability to reproduce the effects of aerodynamic damping.

6.3. Wind Tunnel Tests

In the wave basin experiments, the primary objective is to scrutinize the hydrodynamic response of the platform combined with the emulation of the aerodynamic loads using actuators, thus bypassing the need for a scaled rotor subjected to wind flow. Conversely, wind tunnel testing aims to comprehensively examine the aerodynamic loads, wakes, and turbines' interactions. Within the context of hybrid testing, the motions of the FWT model are simulated using a numerical tool, enabling the replication of the FWT motions through actuators, while a physical rotor is subjected to airflow in the wind tunnel.

Pioneered by researchers from Politecnico de Milano in Italy, a robot of two degrees of freedom (DoF) was developed by Bayati et al. [63] to mimic surge and pitch motions effectively in real-time. The actuator's technical details are documented in [129,130]. The initial application of this robot involved exclusively imposing surge motions upon a scaled 1:75 model of the DTU 10 MW turbine during wind tunnel tests, facilitating a comprehensive exploration of wakes in both steady and unsteady wind conditions [131]. Subsequent enhancements to the robot resulted in the realization of additional degrees of freedom, thus evolving into a six-DoF mechanism (Figure 8) with the name "HexaFloat" [64]. This upgraded robot is then deployed in wind tunnel testing of the DTU 10 MW turbine to represent a floating support platform, as reported in the works of Bayati et al. [132] and Belloli et al. [133]. The presented robot has been utilized for various purposes within the field of wind energy research. Fontanella et al. [134] employed it to investigate the unsteady aerodynamics of the DTU 10 MW WT under imposed surge motions. Additionally, it is utilized in the COREWIND project to examine the aerodynamics of two 15 MW FWTs [135]. Furthermore, the same robot is used in phase III of the OC6 project to collect data for validating the aerodynamic loading on the rotor in motion caused by a floating support structure [136].

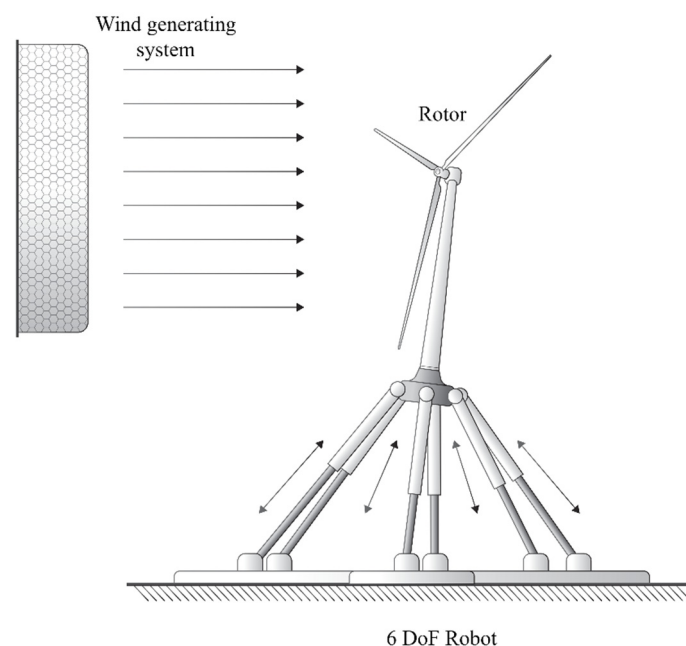


Figure 8. Hybrid testing in the wind tunnel with a 6 DoF robot.

In parallel work, Schliffke et al. [137] embarked upon a similar approach to scrutinize the repercussions of surge motions on wake characteristics. Their experimental campaign involved the utilization of the FLOATGEN barge, integrated with a 2 MW wind turbine, as the focal test model. Instead of deploying a scaled rotor, their concept entailed a porous disc. The imposition of surge displacements is achieved through a motor controlled by the manufacturer's software. Although a modest time delay between the assigned and emulated motion was noted, its effects were deemed negligible, primarily due to its independence from the imposed frequency and amplitude. Notably, their study focused predominantly on the ramifications of surge motion on wake characteristics without delving extensively into motion dynamics. Furthermore, Rockel et al. [138,139] conducted a series of hybrid tests in wind tunnels to ascertain the impact of pitch motions on FWT wakes and the intricate interplay between wakes and the FWT.

7. Methods Comparison and Applicability

7.1. Hybrid vs. Physical Rotor Testing

Hybrid testing conducted in wave basins offers the advantage of not requiring a physical wind generating system; alongside the measured motions, a wind input file is incorporated into the numerical simulation to introduce the wind turbulence during the tests. Additionally, it is possible to emulate the effects of the blade pitch controller and aerodynamic damping as they are included in the simulation results. For PSR, incorporating low-Reynolds modifications poses challenges in accurately modelling the turbine's power coefficient and torque characteristics. This limitation hinders the scalability of blade pitch control and impedes the precise capture of aerodynamic damping effects [101].

Unlike the limitation of physical rotors, the hybrid approach in the wave basin is not restricted to a specific turbine or scale. Utilizing actuators makes it feasible to replicate the aerodynamic loads of any turbine, making the hybrid technique more cost-effective and time-efficient compared to physical rotor testing. The latter necessitates the construction of a scaled rotor for each turbine design, along with the associated scaling coefficient. Hybrid testing campaigns have demonstrated favourable outcomes by emulating the thrust force accurately and replicating torques and gyroscopic moments. Moreover, hybrid testing grants complete control over the aerodynamics (or hydrodynamics) to better focus on one aspect (i.e., aero or hydro) of the study. Meanwhile, the PSR method showcased superior proficiency in catching unexpected, coupled effects. However, PSR may replicate global aerodynamic phenomena with inferior accuracy compared to the numerical models employed in hybrid testing. This discrepancy arises from partially including scaling effects, such as incorrect torque coefficient and absence of blade pitch control.

In addition, there are challenges associated with hybrid testing, primarily related to delays that can impact the fidelity of the tests. The employed actuators must possess sufficient bandwidth to emulate the assigned load or motions accurately within an appropriate time step [101]. The simulation tool implemented in hybrid testing must provide the calculated load within short time steps, justifying the use of BEM-based tools (i.e., OpenFast) rather than CFD. Moreover, the accuracy of the tests depends on several factors, including the precision of motion tracking measurements and the simulation tool employed. It is acknowledged that certain aerodynamic phenomena (in the case of hybrid testing in wave basins) and hydrodynamic responses (in the case of hybrid testing in wind tunnels) that are not accounted for in the numerical model will not be fully replicated in the experiments. Nevertheless, the existing numerical models may already include most known phenomena. So, the omission of phenomena poses a concern only when exhibiting significant coupling effects, which may happen but is unlikely to be known beforehand.

Furthermore, the calibration of the actuation system is challenging, especially for the one employing multiple emulators. While using multiple actuators allows the reproduction of a broader range of loads (in basin tests) or the mimicry of displacements with multiple degrees of freedom (in tunnel tests), it also introduces complexities and additional sources of uncertainty within the measurements [140]. In other words, more attention is required for

the calibration process of the different actuators as well as the mass and inertia quantities, to effectively mitigate and minimize the error levels in both prototype modelling and load replication.

7.2. Actuators' Suitability in Hybrid Testing

It has been demonstrated that both propellers and cable actuators can effectively emulate the thrust force in hybrid testing. However, propeller systems encounter challenges in replicating the aerodynamic moments, as noted by Otter et al. [59], and incorporating the propellers' torques into force allocation is a complex task [140]. On the other hand, cable actuators excel in reproducing the moments, although the control of cables is comparatively more intricate than that of propellers. Additionally, the cable's frame requires a larger space on the top of the tower, unlike propellers, which occupy a smaller footprint. It is worth noting that the pretension of the cables may affect the results of free decay tests if not performed perfectly, as observed by Sauder et al. [55], whereas conducting free decay tests with turned-off propeller actuators is simpler.

In addition, the square frame required for cable actuators occupies a large area on the tower top. In contrast, propellers are lightweight and occupy a smaller footprint. Consequently, calibrating the tower top masses poses a greater challenge for cable systems. Furthermore, propellers are easily transferable between different basins. In contrast, cables require specialized infrastructure, limiting them to the facility for which they were initially designed.

Due to the high rotational speed of the propellers, undesirable vibrations are induced, whereas cables may excite the attaching frame's natural period. Careful attention must be given to the temperature of the active emulator to prevent burning the propeller's electrical motor or demagnetizing it. When dealing with multi-actuator systems, the interaction between propellers must be considered during the tuning process. The wakes of adjacent propellers can modify the air inflow of others, leading to performance changes of up to 10%, as noted by Urbán and Guanche [60] when tested on a fixed support.

Although, propellers and winches are distinct in how they handle load monitoring. Measuring the load generated by propellers is commonly performed via a load cell attached to the tower top. Inertial loads, which are proportional to acceleration, make real-time controlling of the propeller's thrust difficult. Consequently, propellers are often controlled in an open-loop manner, relying solely on fixed-support thrust calibration and empirical correction factors to address uncertainties such as propeller interactions. On the other hand, cable loads can be readily measured using a load cell for each cable, given their negligible mass. This measurement allows for closed-loop control with feedback algorithms that can promptly correct for uncertainties in real-time. Additionally, winch systems typically possess a higher bandwidth, resulting in shorter time delays, a critical factor for ensuring the accuracy of hybrid testing. Hence, winch systems are generally considered to be more accurate than propellers.

The choice between hybrid testing in wind tunnels or wave basins depends on the specifications of the phenomena under investigation. Hybrid testing in wind tunnels is suitable when studying wakes and turbine interactions, while hybrid testing in wave basins with propellers or cables is preferable when focusing on hydrodynamics. If the thrust loading is considered the dominant load for the tests, a single propeller (or a ducted fan) is recommended. On the other hand, a winch system is more appropriate when replicating the aerodynamic and gyroscopic moments. The high bandwidth of cable actuators makes them the preferred option for replicating 3p, tower and vertical loads.

7.3. Method Selection Roadmap

Evaluating and comparing the different methods based on various criteria can provide valuable insights into their performance and suitability for specific applications. Table 3 recaps this assessment based on the cost, accuracy, and other relevant factors. The PSR method exhibits superior performance in emulating the turbine's unexpected, coupled

effects and surpasses the limitations of the porous disc and FSR methods, which are restricted to scenarios below rated wind speed. However, the PSR method may replicate global aerodynamics less accurately than numerical models used in hybrid testing due to scaling effects, including incorrect torque coefficients and the absence of blade pitch control. Therefore, hybrid testing stands as the sole approach that allows testing and evaluating control strategies.

Table 3. Overview of the experimental methodologies used for FWTs.

Criteria \ Method	Porous Disc	FSR	PSR	Hybrid
Aerodynamic loads	Limited	Limited	Effective	Effective
Blade pitch controller	Infeasible	Infeasible	Limited	Highly apt
Development cost	Medium	High	High	High
Operation cost	Medium	High	High	Low
Versatility	Flexible	Restrictive	Restrictive	Flexible
Scalability	Moderate	Limited	Limited	High

Furthermore, the hybrid approach demonstrates enhanced flexibility and cost-efficiency compared to other techniques. Unlike the PSR and FSR methods, which necessitate the construction of new scaled rotors for each turbine design and scaling factor, the actuators utilized in the hybrid approach can represent different turbine designs. These advantages allow for greater versatility and eliminate the need for costly scaled rotor modifications with each variation in design or scaling. Still, the material used for the hybrid framework may be expensive.

Overall, both the PSR and hybrid techniques serve as effective representations of turbine aerodynamics. The PSR method exhibits higher accuracy in emulating unpredicted aerodynamic characteristics, albeit at a higher operation cost. On the other hand, the hybrid technique offers a cost-effective alternative while still providing a reliable representation of turbine aerodynamics and coupled phenomena. The selection of the testing approach typically hinges on the specific objectives of the tests, as well as a careful balance between budget constraints and fidelity requirements. The choice will depend on a trade-off between financial considerations, the available equipment, and mainly the desired level of accuracy and detail in the results, as summarized in Figure 9 showing an agreement with the conclusion of Otter et al. [101].

In the presence of a wind-generating system in an ocean basin, the PSR method can allow for the investigation of unpredicted coupled effects. Otherwise, hybrid testing allows physical testing on the studied phenomenon, including known coupled effects. Hybrid testing in wind tunnels allows for the investigation of the turbines' interactions and wake effects. When studying the hydrodynamic response of FWTs coupled with the aerodynamics, propeller actuators present an option if the thrust force is the dominant aerodynamic effect in the test case. Propellers can be easily moved between different basins, allowing their use in facilities beyond their original development. On the other hand, when the aerodynamic moments are important and a higher bandwidth is sought, dynamic winches are more suitable actuators.

The classification and recommendations represent the current status of FWT testing campaigns. This review indicates a dominance for hybrid testing in the future with technological advancement and improvements in simulation tools. As larger turbines are targeted (i.e., 20 MW turbines and more), small scaling factors will be needed to construct physical rotors, leading to difficulties in building, calibrating, and fitting the system in the testing facility. Hybrid testing overcomes future scaling barriers from larger turbine sizes by representing the rotor with actuators. The improvements in simulation tools will result in an enhanced fidelity of the emulated loads, thus the capability of hybrid testing to replicate coupling effects.

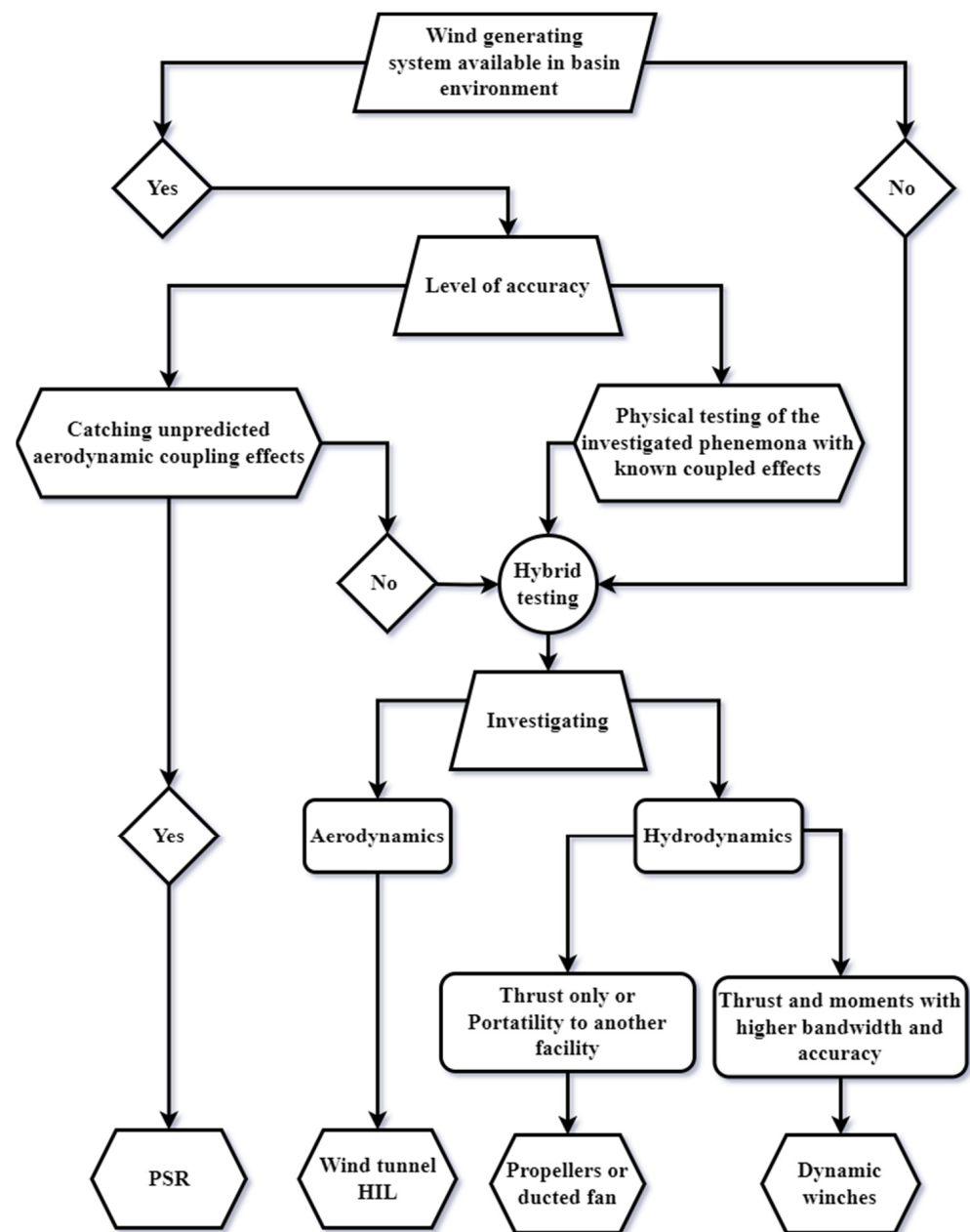


Figure 9. A recommended roadmap for selecting the testing approach.

8. Conclusions

This paper presents a comprehensive review of the experimental methodologies employed in studying FWTs. It begins by summarising the Froude and Reynolds similitude principles and the importance of various aerodynamic phenomena to underscore the associated experimental challenges. Subsequently, the methods are presented, spanning from early-stage techniques like the porous disc method to more contemporary approaches (i.e., the performance scaled rotor (PSR) method and the hybrid approach). Each method is described, providing insights into its specific characteristics, and is evaluated based on criteria such as accuracy, cost, and versatility.

The main emphasis of this review revolves around the assessment of the PSR method and the hybrid approach. The PSR method entails using a redesigned rotor that maintains identical performance characteristics in a lower Reynolds environment. This approach replicates the aerodynamic behaviour of the turbine, including unpredicted coupling effects. However, the introduction of low-Reynolds modifications presents challenges when

attempting to model the power coefficient and torque characteristics of the turbine. Consequently, the scalability of blade pitch control becomes constrained in the PSR approach.

The hybrid approach combines physical experimentation and numerical simulation conducted in wave basins or wind tunnels, with actuators serving as the link between the two in real-time. The hybrid approach proves advantages by simplifying experimental tests in wave basins where a wind generation system is unavailable. Previous hybrid testing campaigns are assessed, specifically focusing on commonly utilized actuators such as cable winches and propellers. The actuation systems are evaluated, emphasizing the simplicity of propellers' calibration compared to cable systems, as well as the cable actuators' capability to reproduce the moments accurately at higher bandwidth. The selection of actuators is discussed, marking its dependence on the investigated phenomena and the targeted fidelity.

It is determined that hybrid testing is versatile, allowing for the evaluation of multiple turbine configurations at different scales. In addition, it provides a reliable representation of turbine aerodynamics and coupled phenomena. On the other hand, the PSR method is recognized for including unpredicted coupling effects while exhibiting lower versatility due to the requirement for costly modifications of scaled rotors with each design variation or scaling.

Based on the presented discussion, a roadmap is outlined for selecting the appropriate methodology, considering the investigated phenomena, level of accuracy, available equipment, and budget constraints. PSR is recommended when a wind-generating system over a wave basin is available, and including unpredicted coupling effects is of concern. Hybrid testing is advised when physically testing the model, including known coupling effects, while giving control on one aspect of the study (aero or hydro). For larger turbines, the hybrid approach is a more promising option in the foreseeable future.

Author Contributions: Conceptualization, M.H., E.U., C.Z., J.F.G. and C.G.S.; methodology, M.H., E.U., C.Z., J.F.G. and C.G.S.; software, M.H., E.U., C.Z., J.F.G. and C.G.S.; validation, M.H., E.U., C.Z., J.F.G. and C.G.S.; formal analysis, M.H., E.U., C.Z., J.F.G. and C.G.S.; investigation, M.H., E.U., C.Z., J.F.G. and C.G.S.; resources, M.H., E.U., C.Z., J.F.G. and C.G.S.; data curation, M.H., E.U., C.Z., J.F.G. and C.G.S.; writing—original draft preparation, M.H.; writing—review and editing, M.H., E.U., C.Z., J.F.G. and C.G.S.; visualization, M.H., E.U., C.Z., J.F.G. and C.G.S.; supervision, E.U. and C.G.S.; project administration, C.G.S.; funding acquisition, C.G.S. All authors have read and agreed to the published version of the manuscript.

Funding: M.H., C.Z. and J.F.G. received funding from the project Variable Geometry Wave Energy Conversion System for Floating Platforms (WEC4MUP), which is funded by the Portuguese Foundation for Science and Technology (Fundação para a Ciência e a Tecnologia—FCT) under contract WEC4MUP_PTDC/EME-REN/0242/2020. E.U. received funding from the project ARCWIND—Adaptation and Implementation of Floating Wind Energy Conversion Technology for the Atlantic Region—which is co-financed by the European Regional Development Fund through the Interreg Atlantic Area Programme under contract EAPA 344/2016. This work contributed to the Strategic Research Plan of the Centre for Marine Technology and Ocean Engineering (CENTEC), which is financed by the Portuguese Foundation for Science and Technology (Fundação para a Ciência e Tecnologia—FCT) under contract UIDB/UIDP/00134/2020.

Institutional Review Board Statement: Not applicable.

Informed Consent Statement: Not applicable.

Data Availability Statement: Not applicable.

Conflicts of Interest: The authors declare no conflict of interest.

References

1. Díaz, H.; Guedes Soares, C. Review of the Current Status, Technology and Future Trends of Offshore Wind Farms. *Ocean. Eng.* **2020**, *209*, 107381. [[CrossRef](#)]
2. Díaz, H.; Serna, J.; Nieto, J.; Guedes Soares, C. Market Needs, Opportunities and Barriers for the Floating Wind Industry. *J. Mar. Sci. Eng.* **2022**, *10*, 934. [[CrossRef](#)]
3. Wind Europe. *Wind Energy in Europe—Statistics and the Outlook for 2021–2025*; WindEurope: Brussels, Belgium, 2021; p. 36.
4. Bagbanci, H.; Karmakar, D.; Guedes Soares, C. Review of Offshore Floating Wind Turbines Concepts. In *Maritime Engineering and Technology*; Guedes Soares, C., Garbatov, Y., Sutulo, S., Santos, T.A., Eds.; Taylor & Francis Group: London, UK, 2012; pp. 553–562. [[CrossRef](#)]
5. Uzunoglu, E.; Guedes Soares, C. Hydrodynamic Design of a Free-Float Capable Tension Leg Platform for a 10 MW Wind Turbine. *Ocean. Eng.* **2020**, *197*, 106888. [[CrossRef](#)]
6. Damiani, R.; Dykes, K.; Scott, G. A Comparison Study of Offshore Wind Support Structures with Monopiles and Jackets for U.S. Waters. *J. Phys. Conf. Ser.* **2016**, *753*, 092003. [[CrossRef](#)]
7. Castro-Santos, L.; Silva, D.; Bento, A.R.; Salvação, N.; Guedes Soares, C. Economic Feasibility of Floating Offshore Wind Farms in Portugal. *Ocean. Eng.* **2020**, *207*, 107393. [[CrossRef](#)]
8. Castro-Santos, L.; Bento, A.R.; Silva, D.; Salvação, N.; Guedes Soares, C. Economic Feasibility of Floating Offshore Wind Farms in the North of Spain. *J. Mar. Sci. Eng.* **2020**, *8*, 58. [[CrossRef](#)]
9. Uzunoglu, E.; Karmakar, D.; Guedes Soares, C. Floating Offshore Wind Platforms. In *Floating Offshore Wind Farms*; Castro-Santos, L., Diaz-Casas, V., Eds.; Green Energy and Technology; Springer International Publishing: Cham, Switzerland, 2016; pp. 53–76. [[CrossRef](#)]
10. Collu, M.; Borg, M. Design of Floating Offshore Wind Turbines. In *Offshore Wind Farms*; Elsevier: Amsterdam, The Netherlands, 2016; pp. 359–385. ISBN 978-0-08-100779-2.
11. Skaare, B.; Nielsen, F.G.; Hanson, T.D.; Yttervik, R.; Havmøller, O.; Rekdal, A. Analysis of Measurements and Simulations from the Hywind Demo Floating Wind Turbine. *Wind Energy* **2015**, *18*, 1105–1122. [[CrossRef](#)]
12. Roddier, D.; Cermelli, C.; Aubault, A.; Weinstein, A. WindFloat: A Floating Foundation for Offshore Wind Turbines. *J. Renew. Sustain. Energy* **2010**, *2*, 033104. [[CrossRef](#)]
13. Reynaud, M.; Le Bouhris, E.; Soulard, T.; Yves, P. *Rapport de Suivi Environnemental de L'éolienne Flottante FLOATGEN, Site D'essais SEM-REV*; Zenodo: Genève, Switzerland, 2021. [[CrossRef](#)]
14. Galván, J.; Sánchez-Lara, M.J.; Mendikoa, I.; Pérez-Morán, G.; Nava, V.; Rodríguez-Arias, R. NAUTILUS-DTU10 MW Floating Offshore Wind Turbine at Gulf of Maine: Public Numerical Models of an Actively Ballasted Semisubmersible. *J. Phys. Conf. Ser.* **2018**, *1102*, 012015. [[CrossRef](#)]
15. Pegalajar-Jurado, A.; Bredmose, H.; Borg, M.; Straume, J.G.; Landbø, T.; Andersen, H.S.; Yu, W.; Müller, K.; Lemmer, F. State-of-the-Art Model for the LIFES50+ OO-Star Wind Floater Semi 10 MW Floating Wind Turbine. *J. Phys. Conf. Ser.* **2018**, *1104*, 012024. [[CrossRef](#)]
16. Borisade, F.; Koch, C.; Lemmer, F.; Cheng, P.W.; Campagnolo, F.; Matha, D. Validation of INNWIND.EU Scaled Model Tests of a Semisubmersible Floating Wind Turbine. *Int. J. Offshore Polar Eng.* **2018**, *28*, 54–64. [[CrossRef](#)]
17. Hmedi, M.; Uzunoglu, E.; Medina-Manuel, A.; Mas-Soler, J.; Vittori, F.; Pires, O.; Azcona, J.; Souto-Iglesias, A.; Guedes Soares, C. Experimental Analysis of CENTEC-TLP Self-Stable Platform with a 10 MW Turbine. *J. Mar. Sci. Eng.* **2022**, *10*, 1910. [[CrossRef](#)]
18. Sanchez, R. *Technology Readiness Assessment Guide*; United States Department of Energy: Washington, DC, USA, 2011; p. 73.
19. ITTC. Recommended Procedures and Guidelines: Model Tests for Offshore Wind Turbines; Recommended Procedures and Guidelines 7.5-02-07-03.8. In Proceedings of the International Towing Tank Conference, Zürich, Switzerland, 13–18 June 2021; p. 19.
20. Uzunoglu, E.; Guedes Soares, C. Parametric Modelling of Marine Structures for Hydrodynamic Calculations. *Ocean. Eng.* **2018**, *160*, 181–196. [[CrossRef](#)]
21. Uzunoglu, E.; Guedes Soares, C. A System for the Hydrodynamic Design of Tension Leg Platforms of Floating Wind Turbines. *Ocean. Eng.* **2019**, *171*, 78–92. [[CrossRef](#)]
22. Jonkman, J. The New Modularization Framework for the FAST Wind Turbine CAE Tool. In Proceedings of the 51st AIAA Aerospace Sciences Meeting Including the New Horizons Forum and Aerospace Exposition, Grapevine (Dallas/Ft. Worth Region), TX, USA, 7–10 January 2013; American Institute of Aeronautics and Astronautics: Grapevine (Dallas/Ft. Worth Region), TX, USA, 2013. [[CrossRef](#)]
23. Perez-Becker, S.; Saverin, J.; Behrens de Luna, R.; Papi, F.; Combreau, C.; Ducasse, M.-L.; Marten, D.; Bianchini, A. *Deliverable 2.2—Validation Report of QBlade-Ocean*; Zenodo: Genève, Switzerland, 2022. [[CrossRef](#)]
24. Chen, P.; Chen, J.; Hu, Z. Review of Experimental-Numerical Methodologies and Challenges for Floating Offshore Wind Turbines. *J. Mar. Sci. Appl.* **2020**, *19*, 339–361. [[CrossRef](#)]
25. Sarpkaya, T. *Wave Forces on Offshore Structures*; Cambridge University Press: Cambridge, UK; New York, NY, USA, 2010; ISBN 978-0-521-89625-2.
26. Chakrabarti, S.K. Physical Modelling of Offshore Structures. In *Handbook of Offshore Engineering*; Elsevier: Amsterdam, The Netherlands, 2005; pp. 1001–1054. ISBN 978-0-08-044381-2.
27. Faltinsen, O.M. *Sea Loads on Ships and Offshore Structures*; Cambridge ocean technology series; Cambridge University Press: Cambridge, UK, 1999; ISBN 978-0-521-45870-2.

28. Müller, K.; Sandner, F.; Bredmose, H.; Azcona, J.; Manjock, A.; Pereira, R. Improved Tank Test Procedures for Scaled Floating Offshore Wind Turbines. In Proceedings of the International Wind Engineering Conference, IWEC 2014, Hannover, Germany, 3–5 September 2014. [[CrossRef](#)]
29. Pao, L.Y.; Johnson, K.E. Control of Wind Turbines. *IEEE Control Syst.* **2011**, *31*, 44–62. [[CrossRef](#)]
30. Jonkman, J. Influence of Control on the Pitch Damping of a Floating Wind Turbine. In Proceedings of the 46th AIAA Aerospace Sciences Meeting and Exhibit, Reno, NV, USA, 7–10 January 2008; American Institute of Aeronautics and Astronautics: Reno, NV, USA, 2008. [[CrossRef](#)]
31. Nielsen, F.G.; Hanson, T.D.; Skaare, B. Integrated Dynamic Analysis of Floating Offshore Wind Turbines. In Proceedings of the 25th International Conference on Offshore Mechanics and Arctic Engineering, Hamburg, Germany, 4–9 June 2006; ASMEDC: Hamburg, Germany, 2006; pp. 671–679. [[CrossRef](#)]
32. Larsen, T.J.; Hanson, T.D. A Method to Avoid Negative Damped Low Frequent Tower Vibrations for a Floating, Pitch Controlled Wind Turbine. *J. Phys. Conf. Ser.* **2007**, *75*, 012073. [[CrossRef](#)]
33. Skaare, B.; Hanson, T.D.; Nielsen, F.G.; Yttervik, R.; Hansen, A.M.; Thomsen, K.; Larsen, T.J. Integrated Dynamic Analysis of Floating Offshore Wind Turbines. In Proceedings of the European Wind Energy Conference and Exhibition, Milan, Italy, 7–10 May 2007.
34. Namik, H.; Stol, K. A Review of Floating Wind Turbine Controllers. In *Handbook of Wind Power Systems*; Pardalos, P.M., Rebennack, S., Pereira, M.V.F., Iliadis, N.A., Pappu, V., Eds.; Energy Systems; Springer: Berlin/Heidelberg, Germany, 2013; pp. 415–441. ISBN 978-3-642-41080-2.
35. Yu, W.; Lemmer, F.; Bredmose, H.; Borg, M.; Pegalajar-Jurado, A.; Mikkelsen, R.F.; Larsen, T.S.; Fjelstrup, T.; Lomholt, A.K.; Boehm, L.; et al. The Triple Spar Campaign: Implementation and Test of a Blade Pitch Controller on a Scaled Floating Wind Turbine Model. *Energy Procedia* **2017**, *137*, 323–338. [[CrossRef](#)]
36. Zhu, H.; Sueyoshi, M. Experimental Study and Attitude Control of a Floating Type Shrouded Wind Turbine. *Sustain. Energy Technol. Assess.* **2022**, *50*, 101811. [[CrossRef](#)]
37. Hu, R.; Le, C.; Gao, Z.; Ding, H.; Zhang, P. Implementation and Evaluation of Control Strategies Based on an Open Controller for a 10 MW Floating Wind Turbine. *Renew. Energy* **2021**, *179*, 1751–1766. [[CrossRef](#)]
38. Utsunomiya, T.; Sato, T.; Matsukuma, H.; Yago, K. Experimental Validation for Motion of a SPAR-Type Floating Offshore Wind Turbine Using 1/22.5 Scale Model. In Proceedings of the ASME 2009 28th International Conference on Ocean, Offshore and Arctic Engineering, Honolulu, HI, USA, 31 May–5 June 2009; ASMEDC: Honolulu, HI, USA, 2009; pp. 951–959. [[CrossRef](#)]
39. Cermelli, C.; Roddier, D.; Aubault, A. WindFloat: A Floating Foundation for Offshore Wind Turbines—Part II: Hydrodynamics Analysis. In Proceedings of the ASME 2009 28th International Conference on Ocean, Offshore and Arctic Engineering, Honolulu, HI, USA, 31 May–5 June 2009; ASMEDC: Honolulu, HI, USA, 2009; pp. 135–143. [[CrossRef](#)]
40. Cermelli, C.; Aubault, A.; Roddier, D.; McCoy, T. Qualification of a Semi-Submersible Floating Foundation for Multi-Megawatt Wind Turbines. In Proceedings of the Offshore Technology Conference, Houston, TX, USA, 3–6 May 2010; OTC-20674-MS. [[CrossRef](#)]
41. Wan, L.; Gao, Z.; Moan, T. Experimental and Numerical Study of Hydrodynamic Responses of a Combined Wind and Wave Energy Converter Concept in Survival Modes. *Coast. Eng.* **2015**, *104*, 151–169. [[CrossRef](#)]
42. Robertson, A.N.; Jonkman, J.M.; Goupee, A.J.; Coulling, A.J.; Prowell, I.; Browning, J.; Masciola, M.D.; Molta, P. Summary of Conclusions and Recommendations Drawn from the DeepCwind Scaled Floating Offshore Wind System Test Campaign. In Proceedings of the ASME 2013 32nd International Conference on Ocean, Offshore and Arctic Engineering, Nantes, France, 9–14 June 2013; American Society of Mechanical Engineers: Nantes, France, 2013; V008T09A053. [[CrossRef](#)]
43. Michailides, C.; Gao, Z.; Moan, T. Experimental and Numerical Study of the Response of the Offshore Combined Wind/Wave Energy Concept SFC in Extreme Environmental Conditions. *Mar. Struct.* **2016**, *50*, 35–54. [[CrossRef](#)]
44. Goupee, A.J.; Koo, B.J.; Kimball, R.W.; Lambrakos, K.F.; Dagher, H.J. Experimental Comparison of Three Floating Wind Turbine Concepts. *J. Offshore Mech. Arct. Eng.* **2014**, *136*, 020906. [[CrossRef](#)]
45. Pegalajar-Jurado, A.; Hansen, A.M.; Laugesen, R.; Mikkelsen, R.F.; Borg, M.; Kim, T.; Heilskov, N.F.; Bredmose, H. Experimental and Numerical Study of a 10MW TLP Wind Turbine in Waves and Wind. *J. Phys. Conf. Ser.* **2016**, *753*, 092007. [[CrossRef](#)]
46. de Ridder, E.-J.; Otto, W.; Zondervan, G.-J.; Huijs, F.; Vaz, G. Development of a Scaled-Down Floating Wind Turbine for Offshore Basin Testing. In Proceedings of the ASME 2014 33rd International Conference on Ocean, Offshore and Arctic Engineering, San Francisco, CA, USA, 8–13 June 2014; American Society of Mechanical Engineers: San Francisco, CA, USA, 2014; V09AT09A027. [[CrossRef](#)]
47. Duan, F.; Hu, Z.; Niedzwecki, J.M. Model Test Investigation of a Spar Floating Wind Turbine. *Mar. Struct.* **2016**, *49*, 76–96. [[CrossRef](#)]
48. Du, W.; Zhao, Y.; He, Y.; Liu, Y. Design, Analysis and Test of a Model Turbine Blade for a Wave Basin Test of Floating Wind Turbines. *Renew. Energy* **2016**, *97*, 414–421. [[CrossRef](#)]
49. Duan, F.; Hu, Z.; Liu, G.; Wang, J. Experimental Comparisons of Dynamic Properties of Floating Wind Turbine Systems Based on Two Different Rotor Concepts. *Appl. Ocean. Res.* **2016**, *58*, 266–280. [[CrossRef](#)]

50. Fowler, M.J.; Kimball, R.W.; Thomas, D.A.; Goupee, A.J. Design and Testing of Scale Model Wind Turbines for Use in Wind/Wave Basin Model Tests of Floating Offshore Wind Turbines. In Proceedings of the ASME 2013 32nd International Conference on Ocean, Offshore and Arctic Engineering, Nantes, France, 9–14 June 2013; American Society of Mechanical Engineers: Nantes, France, 2013; V008T09A00. [[CrossRef](#)]
51. Wen, B.; Tian, X.; Dong, X.; Li, Z.; Peng, Z.; Zhang, W.; Wei, K. Design Approaches of Performance-Scaled Rotor for Wave Basin Model Tests of Floating Wind Turbines. *Renew. Energy* **2020**, *148*, 573–584. [[CrossRef](#)]
52. Gueydon, S.; Lindeboom, R.; Van Kampen, W.; De Ridder, E.-J. Comparison of Two Wind Turbine Loading Emulation Techniques Based on Tests of a TLP-FOWT in Combined Wind, Waves and Current. In Proceedings of the ASME 2018 1st International Offshore Wind Technical Conference, San Francisco, CA, USA, 4–7 November 2018; American Society of Mechanical Engineers: San Francisco, CA, USA, 2018; V001T01A012. [[CrossRef](#)]
53. Arnal, V.; Bonnefoy, F.; Gilloteaux, J.-C.; Aubrun, S. Hybrid Model Testing of Floating Wind Turbines: Test Bench for System Identification and Performance Assessment. In Proceedings of the ASME 2019 38th International Conference on Ocean, Offshore and Arctic Engineering, Glasgow, UK, 9–14 June 2019; American Society of Mechanical Engineers: Glasgow, UK, 2019. [[CrossRef](#)]
54. Azcona, J.; Bouchotrouch, F.; González, M.; Garcíandía, J.; Munduate, X.; Kelberlau, F.; Nygaard, T.A. Aerodynamic Thrust Modelling in Wave Tank Tests of Offshore Floating Wind Turbines Using a Ducted Fan. *J. Phys. Conf. Ser.* **2014**, *524*, 012089. [[CrossRef](#)]
55. Sauder, T.; Chabaud, V.; Thys, M.; Bachynski, E.E.; Sæther, L.O. Real-Time Hybrid Model Testing of a Braceless Semi-Submersible Wind Turbine: Part I—The Hybrid Approach. In Proceedings of the ASME 2016 35th International Conference on Ocean, Offshore and Arctic Engineering, Busan, Republic of Korea, 19–24 June 2016; American Society of Mechanical Engineers: Busan, Republic of Korea, 2016; V006T09A039. [[CrossRef](#)]
56. Bachynski, E.E.; Thys, M.; Sauder, T.; Chabaud, V.; Sæther, L.O. Real-Time Hybrid Model Testing of a Braceless Semi-Submersible Wind Turbine: Part II—Experimental Results. In Proceedings of the ASME 2016 35th International Conference on Ocean, Offshore and Arctic Engineering, Busan, Republic of Korea, 19–24 June 2016; American Society of Mechanical Engineers: Busan, Republic of Korea, 2016; V006T09A040. [[CrossRef](#)]
57. Berthelsen, P.A.; Bachynski, E.E.; Karimirad, M.; Thys, M. Real-Time Hybrid Model Tests of a Braceless Semi-Submersible Wind Turbine: Part III—Calibration of a Numerical Model. In Proceedings of the ASME 2016 35th International Conference on Ocean, Offshore and Arctic Engineering, Busan, Republic of Korea, 19–24 June 2016; American Society of Mechanical Engineers: Busan, Republic of Korea, 2016; V006T09A047. [[CrossRef](#)]
58. Chabaud, V.; Eliassen, L.; Thys, M.; Sauder, T. Multiple-Degree-of-Freedom Actuation of Rotor Loads in Model Testing of Floating Wind Turbines Using Cable-Driven Parallel Robots. *J. Phys. Conf. Ser.* **2018**, *1104*, 012021. [[CrossRef](#)]
59. Otter, A.; Murphy, J.; Desmond, C.J. Emulating Aerodynamic Forces and Moments for Hybrid Testing of Floating Wind Turbine Models. *J. Phys. Conf. Ser.* **2020**, *1618*, 032022. [[CrossRef](#)]
60. Urbán, A.M.; Guanche, R. Wind Turbine Aerodynamics Scale-Modeling for Floating Offshore Wind Platform Testing. *J. Wind. Eng. Ind. Aerodyn.* **2019**, *186*, 49–57. [[CrossRef](#)]
61. Vittori, F.; Bouchotrouch, F.; Lemmer, F.; Azcona, J. Hybrid Scaled Testing of a 5 MW Floating Wind Turbine Using the SiL Method Compared with Numerical Models. In Proceedings of the ASME 2018 37th International Conference on Ocean, Offshore and Arctic Engineering, Madrid, Spain, 17–22 June 2018; American Society of Mechanical Engineers: Madrid, Spain, 2018; V010T09A082. [[CrossRef](#)]
62. Vittori, F.; Pires, O.; Azcona, J.; Uzunoglu, E.; Guedes Soares, C.; Zamora Rodríguez, R.; Souto-Iglesias, A. Hybrid Scaled Testing of a 10 MW TLP Floating Wind Turbine Using the SiL Method to Integrate the Rotor Thrust and Moments. In *Developments in Renewable Energies Offshore*; Guedes Soares, C., Ed.; Taylor & Francis Group: London, UK, 2020; pp. 417–423. [[CrossRef](#)]
63. Bayati, I.; Belloli, M.; Facchinetti, A.; Giappino, S. Wind Tunnel Tests on Floating Offshore Wind Turbines: A Proposal for Hardware-in-the-Loop Approach to Validate Numerical Codes. *Wind. Eng.* **2013**, *37*, 557–568. [[CrossRef](#)]
64. Bayati, I.; Belloli, M.; Ferrari, D.; Fossati, F.; Giberti, H. Design of a 6-DoF Robotic Platform for Wind Tunnel Tests of Floating Wind Turbines. *Energy Procedia* **2014**, *53*, 313–323. [[CrossRef](#)]
65. Bayati, I.; Belloli, M.; Bernini, L.; Fiore, E.; Giberti, H.; Zasso, A. On the Functional Design of the DTU10 MW Wind Turbine Scale Model of LIFES50+ Project. *J. Phys. Conf. Ser.* **2016**, *753*, 052018. [[CrossRef](#)]
66. Bredmose, H.; Larsen, S.; Matha, D.; Rettenmeier, A.; Marino, E.; Sætran, L. *Collation of Offshore Wind Wave Dynamics: Marine Renewables Infrastructure Network for Emerging Energy Technologies D2.4*; DTU: Lyngby, Denmark, 2012.
67. Hall, M.; Moreno, J.; Thiagarajan, K. Performance Specifications for Real-Time Hybrid Testing of 1:50-Scale Floating Wind Turbine Models. In Proceedings of the ASME 2014 33rd International Conference on Ocean, Offshore and Arctic Engineering, San Francisco, CA, USA, 8–13 June 2014; American Society of Mechanical Engineers: San Francisco, CA, USA, 2014; V09BT09A047. [[CrossRef](#)]
68. Coulling, A.J.; Goupee, A.J.; Robertson, A.N.; Jonkman, J.M.; Dagher, H.J. Validation of a FAST Semi-Submersible Floating Wind Turbine Numerical Model with DeepCwind Test Data. *J. Renew. Sustain. Energy* **2013**, *5*, 023116. [[CrossRef](#)]
69. Blusseau, P.; Patel, M.H. Gyroscopic Effects on a Large Vertical Axis Wind Turbine Mounted on a Floating Structure. *Renew. Energy* **2012**, *46*, 31–42. [[CrossRef](#)]
70. Bachynski, E.E.; Chabaud, V.; Sauder, T. Real-Time Hybrid Model Testing of Floating Wind Turbines: Sensitivity to Limited Actuation. *Energy Procedia* **2015**, *80*, 2–12. [[CrossRef](#)]

71. Goupee, A.J.; Kimball, R.W.; Dagher, H.J. Experimental Observations of Active Blade Pitch and Generator Control Influence on Floating Wind Turbine Response. *Renew. Energy* **2017**, *104*, 9–19. [[CrossRef](#)]
72. Namik, H.; Stol, K. Individual Blade Pitch Control of Floating Offshore Wind Turbines. *Wind Energy* **2010**, *13*, 74–85. [[CrossRef](#)]
73. Manwell, J.F.; McGowan, J.G.; Rogers, A.L. *Wind Energy Explained: Theory, Design and Application*, 2nd ed.; Wiley: Chichester, UK, 2009; ISBN 978-0-470-01500-1.
74. Bahramiasl, S.; Abbaspour, M.; Karimirad, M. Experimental Study on Gyroscopic Effect of Rotating Rotor and Wind Heading Angle on Floating Wind Turbine Responses. *Int. J. Environ. Sci. Technol.* **2018**, *15*, 2531–2544. [[CrossRef](#)]
75. Høeg, C.E.; Zhang, Z. The Influence of Gyroscopic Effects on Dynamic Responses of Floating Offshore Wind Turbines in Idling and Operational Conditions. *Ocean. Eng.* **2021**, *227*, 108712. [[CrossRef](#)]
76. Arnal, V. Experimental Modelling of a Floating Wind Turbine Using a “Software-in-the-Loop” Approach. Ph.D. Thesis, Ecole Central Nantes, Nantes, France, 2020.
77. Tomasicchio, G.R.; D’Alessandro, F.; Avossa, A.M.; Riefolo, L.; Musci, E.; Ricciardelli, F.; Vicinanza, D. Experimental Modelling of the Dynamic Behaviour of a Spar Buoy Wind Turbine. *Renew. Energy* **2018**, *127*, 412–432. [[CrossRef](#)]
78. Wan, L.; Gao, Z.; Moan, T.; Lugni, C. Experimental and Numerical Comparisons of Hydrodynamic Responses for a Combined Wind and Wave Energy Converter Concept under Operational Conditions. *Renew. Energy* **2016**, *93*, 87–100. [[CrossRef](#)]
79. Wan, L.; Greco, M.; Lugni, C.; Gao, Z.; Moan, T. A Combined Wind and Wave Energy-Converter Concept in Survival Mode: Numerical and Experimental Study in Regular Waves with a Focus on Water Entry and Exit. *Appl. Ocean. Res.* **2017**, *63*, 200–216. [[CrossRef](#)]
80. Mortensen, S.M.; Laugesen, K.; Jensen, J.K.; Jessen, K.; Soltani, M. Experimental Verification of the Hydro-Elastic Model of a Scaled Floating Offshore Wind Turbine. In Proceedings of the 2018 IEEE Conference on Control Technology and Applications (CCTA), Copenhagen, Denmark, 21–24 August 2018; IEEE: Copenhagen, Denmark, 2018; pp. 1623–1630. [[CrossRef](#)]
81. Ahn, H.-J.; Shin, H. Model Test and Numerical Simulation of OC3 Spar Type Floating Offshore Wind Turbine. *Int. J. Nav. Archit. Ocean. Eng.* **2019**, *11*, 1–10. [[CrossRef](#)]
82. Wen, B.; Jiang, Z.; Li, Z.; Peng, Z.; Dong, X.; Tian, X. On the Aerodynamic Loading Effect of a Model Spar-Type Floating Wind Turbine: An Experimental Study. *Renew. Energy* **2022**, *184*, 306–319. [[CrossRef](#)]
83. Martin, H.R.; Kimball, R.W.; Viselli, A.M.; Goupee, A.J. Methodology for Wind/Wave Basin Testing of Floating Offshore Wind Turbines. *J. Offshore Mech. Arct. Eng.* **2014**, *136*, 020905. [[CrossRef](#)]
84. Tracy, C.H. Parametric Design of Floating Wind Turbines. Ph.D. Thesis, Massachusetts Institute of Technology, Cambridge, MA, USA, 2007.
85. Jonkman, J. *Definition of the Floating System for Phase IV of OC3*; NREL: Golden, CO, USA, 2010; NREL/TP-500-47535, 979456.
86. Robertson, A.; Jonkman, J.; Masciola, M.; Song, H.; Goupee, A.; Coulling, A.; Luan, C. *Definition of the Semisubmersible Floating System for Phase II of OC4*; NREL: Golden, CO, USA, 2014; NREL/TP-5000-60601, 1155123.
87. Jonkman, J.; Prowell, I.; Robertson, A.; Goupee, A.J.; Stewart, G.M. Numerical Prediction of Experimentally Observed Behavior of a Scale-Model of an Offshore Wind Turbine Supported by a Tension-Leg Platform. In Proceedings of the Offshore Technology Conference, Houston, TX, USA, 6–9 May 2013; OTC: Houston, TX, USA, 2013; OTC-24233-MS. [[CrossRef](#)]
88. Browning, J.R.; Jonkman, J.; Robertson, A.; Goupee, A.J. Calibration and Validation of a Spar-Type Floating Offshore Wind Turbine Model Using the FAST Dynamic Simulation Tool. *J. Phys. Conf. Ser.* **2014**, *555*, 012015. [[CrossRef](#)]
89. Li, L.; Gao, Y.; Hu, Z.; Yuan, Z.; Day, S.; Li, H. Model Test Research of a Semisubmersible Floating Wind Turbine with an Improved Deficient Thrust Force Correction Approach. *Renew. Energy* **2018**, *119*, 95–105. [[CrossRef](#)]
90. Lemmer, F.; Amann, F.; Matha, D.; Armendariz, J.; Munduate, X.; Bottasso, C.; Campagnolo, F.; Montinari, P.; Manjock, A.; Pereira, R.; et al. Model Building and Scaled Testing of 5 MW and 10 MW Semi-Submersible Floating Wind Turbines. In Proceedings of the 12th Deep Sea Offshore Wind R&D Conference, EERA Deep Wind’2015, Trondheim, Norway, 4–6 February 2015.
91. Helder, J.; Pietersma, M. *UMaine-DeepCwind/OC4 Semi Floating Wind Turbine Repeat Tests*; Maritime Research Institute Netherlands: Wageningen, The Netherlands, 2013.
92. Zhao, Y.; She, X.; He, Y.; Yang, J.; Peng, T.; Kou, Y. Experimental Study on New Multi-Column Tension-Leg-Type Floating Wind Turbine. *China Ocean Eng.* **2018**, *32*, 123–131. [[CrossRef](#)]
93. Bak, C.; Zahle, F.; Bitsche, R.; Kim, T.; Yde, A.; Henriksen, L.C.; Hansen, M.H.; Blasques, J.P.A.A.; Gaunaa, M.; Natarajan, A. *The DTU 10-MW Reference Wind Turbine*; DTU: Lyngby, Denmark, 2013.
94. Bredmose, H.; Lemmer, F.; Borg, M.; Pegalajar-Jurado, A.; Mikkelsen, R.F.; Larsen, T.S.; Fjelstrup, T.; Yu, W.; Lomholt, A.K.; Boehm, L.; et al. The Triple Spar Campaign: Model Tests of a 10 MW Floating Wind Turbine with Waves, Wind and Pitch Control. *Energy Procedia* **2017**, *137*, 58–76. [[CrossRef](#)]
95. Bredmose, H.; Robert, M.; Anders Mandrup, H.; Robert, L.; Nicolai, H.; Bjarne, J.; Jens, K. *Experimental Study of the DTU 10 MW Wind Turbine on a TLP Floater in Waves and Wind*; EWEA: Brussels, Belgium, 2015.
96. Azcona, J.; Lemmer, F.; Matha, D.; Amann, F.; Bottasso, C.L.; Montinari, P.; Chassapoyannis, P.; Diakakis, K.; Voutsinas, S.; Pereira, R.; et al. *D4.2.4: Results of Wave Tank Tests*; Deliverable reports on INNWIND.EU; DTU: Delhi, India, 2016; p. 114.
97. Ahn, H.; Shin, H. Experimental and Numerical Analysis of a 10 MW Floating Offshore Wind Turbine in Regular Waves. *Energies* **2020**, *13*, 2608. [[CrossRef](#)]

98. Madsen, F.J.; Nielsen, T.R.L.; Kim, T.; Bredmose, H.; Pegalajar-Jurado, A.; Mikkelsen, R.F.; Lomholt, A.K.; Borg, M.; Mirzaei, M.; Shin, P. Experimental Analysis of the Scaled DTU10MW TLP Floating Wind Turbine with Different Control Strategies. *Renew. Energy* **2020**, *155*, 330–346. [[CrossRef](#)]
99. Connolly, A.; Guyot, M.; Le Boulluec, M.; Héry, L.; O'Connor, A. Fully Coupled Aero-Hydro-Structural Simulation of New Floating Wind Turbine Concept. In Proceedings of the ASME 2018 1st International Offshore Wind Technical Conference, San Francisco, CA, USA, 4–7 November 2018; American Society of Mechanical Engineers: San Francisco, CA, USA, 2018; p. V001T01A027. [[CrossRef](#)]
100. Shroff, S.; Makris, A.; Roukis, G.; Croce, A.; Karakalas, A.; Machairas, T.; Saravanos, D.; Chrysochoidis, N.; Theodosiou, T.; Berring, P.; et al. D2.24: *Manufactured and Laboratory Tested Scaled Blades and Parts of the Blade*; Deliverable reports on INNWIND.EU; DTU: Delhi, India, 2012; p. 150.
101. Otter, A.; Murphy, J.; Pakrashi, V.; Robertson, A.; Desmond, C. A Review of Modelling Techniques for Floating Offshore Wind Turbines. *Wind Energy* **2021**, *25*, 831–857. [[CrossRef](#)]
102. Carrion, J.E.; Spencer, B.F., Jr. *Model-Based Strategies for Real-Time Hybrid Testing*; Newmark Structural Engineering Laboratory Report Series 006; Newmark Structural Engineering Laboratory, University of Illinois at Urbana-Champaign: Champaign, IL, USA, 2007; ISSN 1940-9826.
103. Chabaud, V.; Steen, S.; Skjetne, R. Real-Time Hybrid Testing for Marine Structures: Challenges and Strategies. In Proceedings of the ASME 2013 32nd International Conference on Ocean, Offshore and Arctic Engineering, Nantes, France, 9–14 June 2013; American Society of Mechanical Engineers: Nantes, France, 2013. [[CrossRef](#)]
104. Stewart, G.; Muskulus, M. Aerodynamic Simulation of the MARINTEK Braceless Semisubmersible Wave Tank Tests. *J. Phys. Conf. Ser.* **2016**, *749*, 012012. [[CrossRef](#)]
105. Xu, S.; Ji, C.; Guedes Soares, C. Experimental Study on Taut and Hybrid Moorings Damping and Their Relation with System Dynamics. *Ocean. Eng.* **2018**, *154*, 322–340. [[CrossRef](#)]
106. Ji, C.; Xu, S. Verification of a Hybrid Model Test Method for a Deep Water Floating System with Large Truncation Factor. *Ocean. Eng.* **2014**, *92*, 245–254. [[CrossRef](#)]
107. Stansberg, C.T.; Øritsland, O.; Kleiven, G. VERIDEEP: Reliable Methods for Laboratory Verification of Mooring and Stationkeeping in Deep Water. In Proceedings of the Offshore Technology Conference, Houston, TX, USA, 1–4 May 2000; OTC: Houston, TX, USA, 2000; OTC-12087-MS. [[CrossRef](#)]
108. Stansberg, C.T.; Yttervik, R.; Øritsland, O.; Kleiven, G. Hydrodynamic Model Test Verification of a Floating Platform System in 3000m Water Depth. In Proceedings of the International Conference on Offshore Mechanics and Arctic Engineering, OMAE2000-OFT4145, New Orleans, LA, USA, 14–17 February 2000; Volume 2, pp. 325–334.
109. Ormberg, H.; Stansberg, C.T.; Yttervik, R.; Kleiven, G. Integrated Vessel Motion and Mooring Analysis Applied in Hybrid Model Testing. In Proceedings of the Ninth International Offshore and Polar Engineering Conference, Brest, France, 30 May–4 June 1999; ISOPE-I-99-051.
110. Jonkman, J.; Buhl, M.L., Jr. *FAST User's Guide*; National Renewable Energy Laboratory (NREL): Golden, CO, USA, 2005; p. 143.
111. Azcona, J.; Bouchotrouch, F.; Vittori, F. Low-frequency Dynamics of a Floating Wind Turbine in Wave Tank-Scaled Experiments with SiL Hybrid Method. *Wind Energy* **2019**, *22*, 1402–1413. [[CrossRef](#)]
112. Desmond, C.; Hinrichs, J.-C.; Murphy, J. Uncertainty in the Physical Testing of Floating Wind Energy Platforms' Accuracy versus Precision. *Energies* **2019**, *12*, 435. [[CrossRef](#)]
113. Wright, C.; O'Sullivan, K.; Murphy, J.; Pakrashi, V. Experimental Comparison of Dynamic Responses of a Tension Moored Floating Wind Turbine Platform with and without Spring Dampers. *J. Phys. Conf. Ser.* **2015**, *628*, 012056. [[CrossRef](#)]
114. Andersen, M.T. *Floating Foundations for Offshore Wind Turbines*. Ph.D. Thesis, Aalborg Universitetsforlag, Aalborg, Denmark, 2016.
115. Matoug, C.; Augier, B.; Paillard, B.; Maurice, G.; Sicot, C.; Barre, S. An Hybrid Approach for the Comparison of VAWT and HAWT Performances for Floating Offshore Wind Turbines. *J. Phys. Conf. Ser.* **2020**, *1618*, 032026. [[CrossRef](#)]
116. Achard, J.-L.; Maurice, G.; Balarac, G.; Barre, S. Floating Vertical Axis Wind Turbine—OWLWIND Project. In Proceedings of the 2017 International Conference on ENERGY and ENVIRONMENT (CIEM), Bucharest, Romania, 19–20 October 2017; IEEE: Bucharest, Romania, 2017; pp. 216–220. [[CrossRef](#)]
117. Zamora-Rodriguez, R.; Gomez-Alonso, P.; Amate-Lopez, J.; De-Diego-Martin, V.; Dinoi, P.; Simos, A.N.; Souto-Iglesias, A. Model Scale Analysis of a TLP Floating Offshore Wind Turbine. In Proceedings of the ASME 2014 33rd International Conference on Ocean, Offshore and Arctic Engineering, San Francisco, CA, USA, 8–13 June 2014; American Society of Mechanical Engineers: San Francisco, CA, USA, 2014; V09BT09A016. [[CrossRef](#)]
118. Oguz, E.; Clelland, D.; Day, A.H.; Incecik, A.; López, J.A.; Sánchez, G.; Almeria, G.G. Experimental and Numerical Analysis of a TLP Floating Offshore Wind Turbine. *Ocean. Eng.* **2018**, *147*, 591–605. [[CrossRef](#)]
119. Leroy, V.; Delacroix, S.; Merrien, A.; Bachynski-Polić, E.E.; Gilloteaux, J.-C. Experimental Investigation of the Hydro-Elastic Response of a Spar-Type Floating Offshore Wind Turbine. *Ocean. Eng.* **2022**, *255*, 111430. [[CrossRef](#)]
120. Pires, O.; Azcona, J.; Vittori, F.; Bayati, I.; Gueydon, S.; Fontanella, A.; Liu, Y.; de Ridder, E.J.; Belloli, M.; van Wingerden, J.W. Inclusion of Rotor Moments in Scaled Wave Tank Test of a Floating Wind Turbine Using SiL Hybrid Method. *J. Phys. Conf. Ser.* **2020**, *1618*, 032048. [[CrossRef](#)]

121. Hmedi, M.; Uzunoglu, E.; Guedes Soares, C.; Medina-Manuel, A.; Mas-Soler, J.; Abad-Gibert, V.; Souto-Iglesias, A.; Vittori, F.; Pires, O.; Azcona, J. Experimental Analysis of a Free-Float Capable Tension Leg Platform with a 10 MW Turbine. In *Trends in Renewable Energies Offshore*; Guedes Soares, C., Ed.; Taylor & Francis Group: London, UK, 2022; pp. 549–557. [[CrossRef](#)]
122. Vittori, F.; Azcona, J.; Eguinoa, I.; Pires, O.; Rodríguez, A.; Morató, Á.; Garrido, C.; Desmond, C. Model Tests of a 10 MW Semi-Submersible Floating Wind Turbine under Waves and Wind Using Hybrid Method to Integrate the Rotor Thrust and Moments. *Wind Energy Sci.* **2022**, *7*, 2149–2161. [[CrossRef](#)]
123. Armesto, J.A.; Jurado, A.; Guanche, R.; Couñago, B.; Urbano, J.; Serna, J. TELWIND: Numerical Analysis of a Floating Wind Turbine Supported by a Two Bodies Platform. In Proceedings of the ASME 2018 37th International Conference on Ocean, Offshore and Arctic Engineering, Madrid, Spain, 17–22 June 2018; American Society of Mechanical Engineers: Madrid, Spain, 2018; V010T09A073. [[CrossRef](#)]
124. Otter, A.; Flannery, B.; Murphy, J.; Desmond, C. Current Simulation with Software in the Loop for Floating Offshore Wind Turbines. *J. Phys. Conf. Ser.* **2022**, *2265*, 042028. [[CrossRef](#)]
125. Kanner, S.; Yeung, R.W.; Koukina, E. Hybrid Testing of Model-Scale Floating Wind Turbines Using Autonomous Actuation and Control. In Proceedings of the OCEANS 2016 MTS/IEEE Monterey, Monterey, CA, USA, 19–23 September 2016; IEEE: Monterey, CA, USA, 2016; pp. 1–6. [[CrossRef](#)]
126. Thys, M.; Chabaud, V.; Sauder, T.; Eliassen, L.; Sæther, L.; Magnussen, Ø. Real-Time Hybrid Model Testing of a Semi-Submersible 10 MW Floating Wind Turbine and Advances in the Test Method. In Proceedings of the ASME 2018 1st International Offshore Wind Technical Conference, San Francisco, CA, USA, 4–7 November 2018; American Society of Mechanical Engineers: San Francisco, CA, USA, 2018; V001T01A013. [[CrossRef](#)]
127. Antonutti, R.; Poirier, J.-C.; Gueydon, S. Coupled Testing of Floating Wind Turbines in Waves and Wind Using Winches and Software-in-the-Loop. In Proceedings of the Offshore Technology Conference, Houston, TX, USA, 4–7 May 2020; OTC: Houston, TX, USA, 2020; D021S019R001. [[CrossRef](#)]
128. Hall, M.; Goupee, A.J. Validation of a Hybrid Modeling Approach to Floating Wind Turbine Basin Testing: Validation of a Hybrid Modeling Approach to Floating Wind Turbine Basin Testing. *Wind Energy* **2018**, *21*, 391–408. [[CrossRef](#)]
129. Ambrosini, S.; Bayati, I.; Facchinetti, A.; Belloli, M. Methodological and Technical Aspects of a Two-Degrees-of-Freedom Hardware-In-the-Loop Setup for Wind Tunnel Tests of Floating Systems. *J. Dyn. Syst. Meas. Control* **2020**, *142*, 061002. [[CrossRef](#)]
130. Bayati, I.; Belloli, M.; Facchinetti, A. Wind Tunnel 2-DoF Hybrid/HIL Tests on the OC5 Floating Offshore Wind Turbine. In Proceedings of the ASME 2017 36th International Conference on Ocean, Offshore and Arctic Engineering, Trondheim, Norway, 25–30 June 2017; American Society of Mechanical Engineers: Trondheim, Norway, 2017; V010T09A076. [[CrossRef](#)]
131. Bayati, I.; Belloli, M.; Bernini, L.; Zasso, A. Wind Tunnel Wake Measurements of Floating Offshore Wind Turbines. *Energy Procedia* **2017**, *137*, 214–222. [[CrossRef](#)]
132. Bayati, I.; Facchinetti, A.; Fontanella, A.; Giberti, H.; Belloli, M. A Wind Tunnel/HIL Setup for Integrated Tests of Floating Offshore Wind Turbines. *J. Phys. Conf. Ser.* **2018**, *1037*, 052025. [[CrossRef](#)]
133. Belloli, M.; Bayati, I.; Facchinetti, A.; Fontanella, A.; Giberti, H.; La Mura, F.; Taruffi, F.; Zasso, A. A Hybrid Methodology for Wind Tunnel Testing of Floating Offshore Wind Turbines. *Ocean. Eng.* **2020**, *210*, 107592. [[CrossRef](#)]
134. Fontanella, A.; Bayati, I.; Mikkelsen, R.; Belloli, M.; Zasso, A. UNAFLOW: A Holistic Wind Tunnel Experiment about the Aerodynamic Response of Floating Wind Turbines under Imposed Surge Motion. *Wind. Energy Sci.* **2021**, *6*, 1169–1190. [[CrossRef](#)]
135. Fontanella, A.; Facchinetti, A.; Di Carlo, S.; Belloli, M. Wind Tunnel Investigation of the Aerodynamic Response of Two 15 MW Floating Wind Turbines. *Wind. Energy Sci.* **2022**, *7*, 1711–1729. [[CrossRef](#)]
136. Bergua, R.; Robertson, A.; Jonkman, J.; Branlard, E.; Fontanella, A.; Belloli, M.; Schito, P.; Zasso, A.; Persico, G.; Sanvito, A.; et al. OC6 Project Phase III: Validation of the Aerodynamic Loading on a Wind Turbine Rotor Undergoing Large Motion Caused by a Floating Support Structure. *Wind. Energy Sci.* **2023**, *8*, 465–485. [[CrossRef](#)]
137. Schliffke, B.; Aubrun, S.; Conan, B. Wind Tunnel Study of a “Floating” Wind Turbine’s Wake in an Atmospheric Boundary Layer with Imposed Characteristic Surge Motion. *J. Phys. Conf. Ser.* **2020**, *1618*, 062015. [[CrossRef](#)]
138. Rockel, S.; Camp, E.; Schmidt, J.; Peinke, J.; Cal, R.; Hölling, M. Experimental Study on Influence of Pitch Motion on the Wake of a Floating Wind Turbine Model. *Energies* **2014**, *7*, 1954–1985. [[CrossRef](#)]
139. Rockel, S.; Peinke, J.; Hölling, M.; Cal, R.B. Wake to Wake Interaction of Floating Wind Turbine Models in Free Pitch Motion: An Eddy Viscosity and Mixing Length Approach. *Renew. Energy* **2016**, *85*, 666–676. [[CrossRef](#)]
140. Hmedi, M.; Uzunoglu, E.; Guedes Soares, C. Review of Hybrid Model Testing Approaches for Floating Wind Turbines. In *Trends in Maritime Technology and Engineering*; Guedes Soares, C., Santos, T.A., Eds.; Taylor & Francis Group: London, UK, 2022; Volume 2, pp. 421–428. [[CrossRef](#)]

Disclaimer/Publisher’s Note: The statements, opinions and data contained in all publications are solely those of the individual author(s) and contributor(s) and not of MDPI and/or the editor(s). MDPI and/or the editor(s) disclaim responsibility for any injury to people or property resulting from any ideas, methods, instructions or products referred to in the content.